ALOE-VERA EXTRACT AS DRAG REDUCING POLYMER TO REGULATE BLOOD PRESSURE AND TISSUE OXYGENATION DURING HEMORRHAGIC SHOCK

A THESIS SUBMITTED TO

THE GRADUATE SCHOOL OF

ENGINEERING AND NATURAL SCIENCES

OF ISTANBUL MEDIPOL UNIVERSITY

IN PARTIAL FULFILLMENT OF THE REQUIREMENTS FOR

THE DEGREE OF

MASTER OF SCIENCE

IN

BIOMEDICAL ENGINEERING AND BIOINFORMATICS

by

Gülden AKÇAY

September, 2019

ABSTRACT

ALOE-VERA EXTRACT AS DRAG REDUCING POLYMER TO REGULATE BLOOD PRESSURE AND TISSUE OXYGENATION DURING HEMORRHAGIC SHOCK

Gülden Akçay

M.S. in Biomedical Engineering and Bioinformatics

Advisor: Assoc. Prof. Dr. Yasemin Yüksel Durmaz

September, 2019

Hemorrhagic shock is one of the most important causes of death among traumatized patients. The common treatment is replacing lost volume with colloids or crystalloids, which should never be overloaded to return blood pressure to normal levels, otherwise increasing bleeding may cause mortality. In this study, it is aimed to develop a blood supply product to replace conventional resuscitation during hemorrhagic shock. Drag-reducing polymer (DRP) is blood soluble long chain and high molecular weight polymers. These polymers have a significant effect on blood circulation even if they are added at a very small concentration to the blood. Furthermore, these high molecular weight polymers are capable of reducing the resistance in the vascular system without significantly changing its viscosity. DRPs can contribute to tissue perfusion by reducing the plasma region between the red blood cells and the vessel wall, as well as providing better diffusion of oxygen molecules from the red blood cells into the tissues due to their ability to better mix within the plasma surrounding the red blood cells. In this study, AVDRP (aloe-vera based DRP) was obtained from an aloe-vera plant. Given the fact that DRP has a positive effect on tissue perfusion, AVDRP was modified by the fluorinated alkyl chains (AVDRP/F) to allow dissolving more oxygen in the blood and thus, the effect of tissue perfusion was expected to be enhanced.

Drag reducing ability (DRA) of AVDRP was tested in vitro with the Extracorporeal Membrane Oxygenation (ECMO) system. Since the Reynolds numbers in the arteries in the body are well below 1000, the flow in the microcirculation is not turbulent; ECMO system allows us to create turbulences flow to show DRA effect of AVDRP. To see the effects of DRPs on blood circulation a fixed-pressure hemorrhagic shock model was studied in rabbits. After shock was induced, the animals were resuscitated with Ringer Lactate (RL), commercial DRP polymer (PEG), AVDRP, or AVDRP/F at a ppm level concentration. Mean arterial pressure (MAP) and tissue perfusion were monitored during whole operation. Partial pressure of oxygen (pO_2), partial pressure of carbon dioxide (pCO_2), pH, lactate, saturated oxygen (sO_2) level and other important blood parameters were measured at each time point by blood gas analyzer. Additional saturated oxygen (sO_2) level was also monitored using oxymetry and blood viscosity was measured during whole operation.

The results showed that AVDRP and AVDRP/F have a better ability than RL and PEG to reduce pressure decrease during hemorrhagic shock. During resuscitation these groups were recovered their MAP values more than 90%. They showed higher pO_2 level than control groups. Laser speckle analysis proved that they have better ability to increase tissue perfusion.

ÖZET

SÜRÜKLEME AZALTICI POLİMER OLARAK ALOE-VERA ÖZÜNÜN HEMORAJİK ŞOK SIRASINDA KAN BASINCINI VE DOKU OKSİJENLENMESİNİ DÜZENLEMESİ

Gülden Akçay

Biyomedikal Mühendisliği ve Biyoenformatik, Yüksek Lisans

Tez Danışmanı: Doç. Dr. Yasemin Yüksel Durmaz

Eylül, 2019

Hemorajik şok, travmatize olan hastalar arasında ölümün en önemli nedenlerinden biridir. Yaygın tedavi, kan basıncını normal seviyelere getirmek için asla aşırı yüklenmemesi gereken kolloidler veya kristaloitler ile kaybedilen hacmin değiştirilmesidir, aksi takdirde kanamanın artması mortaliteye neden olabilir. Bu çalışmada, hemorajik şok sırasında geleneksel resüstasyonun yerine kullanılabilmesi için bir kan tedarik ürünü geliştirilmesi amaçlanmıştır. Sürükleme azaltıcı polimer (SAP) yüksek moleküler ağırlıklı ve kanda çözünebilen uzun zincirlerdir, kana çok küçük konsantrasyonlarda eklenseler bile kan dolaşımı üzerinde önemli bir etkiye sahiptirler. Bu yüksek moleküler ağırlıklı polimer, viskoziteyi önemli oranda değiştirmeden vasküler sistemdeki direnci azaltabilir. SAP'lar, kırmızı kan hücreleri ve damar duvarı arasındaki plazma bölgesini azaltmasının yanı sıra kırmızı kan hücrelerini çevreleyen plazma içinde daha iyi karışabilmeleri nedeniyle oksijen moleküllerinin kırmızı kan hücrelerinden dokulara daha iyi difüz olmasını sağlayarak doku perfüzyonuna katkıda bulunurlar. Bu tez çalışmasında, bir aloe-vera bitkisinden AVSAP (aloe-vera bazlı SAP) elde edilerek, hemorajik şok sırasında kan basıncına ve doku perfüzyonuna etkileri incelenmiştir. Kendilerine özgü mekanizmaları ile SAP'ın doku perfüzyonu üzerinde olumlu etkisi, AVSAP'ın kanda daha fazla oksijen çözünmesine imkan verecek şekilde modifiye edilmesi amaçlanmıştır. Floroalkil zincirleri ile

modifiye edilerek elde edilen AVSAP/F polimerinin doku perfüzyonuna etkileri incelenmiştir.

AVSAP'ın sürükleme azaltma yeteneği (SA), Ekstrakorporeal Membran Oksijenlendirme (ECMO) sistemi ile türbülanslı akış oluşturularak *in-vitro* ortamda test edilmiştir. SAP'lerin kan dolaşımı üzerindeki etkileri *in-vivo* olarak tavşanlarda oluşturulan sabit basınçlı hemorajik şok modeli ile incelenmiştir. Hemorajik şok oluşturulan hayvanlar, ppm seviyesinde bir konsantrasyonda ticari SAP polimeri (PEG), AVSAP ve AVSAP/F ile resüsite edilerek MAP ve doku perfüzyonu değerleri kontrol grubu olarak Ringer Laktat (RL) ile kıyaslanmışlardır. Kısmi oksijen basıncı (pO_2), kısmi karbondioksit basıncı (pCO_2), pH, laktat, doymuş oksijen (sO2) seviyesi ve diğer önemli kan parametreleri, belirli zaman aralıklarında kan gazı analiz cihazı ile ölçülmüştür. Ek olarak, doymuş oksijen (sO_2) seviyesi de oksimetri kullanılarak izlenmiş, kan viskozite değeri de viskozimetre yardımıyla ölçülmüştür. Elde edilen sonuçlar AVSAP ve AVSAP/F'nin hemorajik şok sırasında basınç düşüşünü azaltmada daha iyi performans sergilediklerini göstermiştir. Resüstasyon sırasında bu gruplarda hem MAP değerleri % 90'ten fazla geri kazanılmış hem de kontrol grubuna kıyasla daha yüksek pO_2 seviyesine erişilmiştir. Ayrıca, lazer benek analizi, doku perfüzyonunu arttırmada daha iyi olduklarını kanıtlamıştır.

Anahtar sözcükler: Hemorajik şok, sürükleme azaltıcı polimer (SAP), resüstasyon ajanı, kan basıncı, oksijen taşıma, tavşanda hemorajik şok modeli

Acknowledgment

Foremost, I would like to express my sincere gratitude to my advisor Assoc. Prof. Dr. Yasemin Yüksel Durmaz of my master's study and research, for his patience, motivation, enthusiasm, and immense knowledge. The door to her office was always open whenever I ran into a trouble spot or had a question about my research or writing. She consistently steered me in the right direction whenever she thought I needed it. I could not have imagined having a better advisor and mentor for my educational journey.

Besides my advisor, I would like to thank the rest of my thesis committee: Asst. Prof. Dr. Mehmet Kocatürk and Assoc. Prof. Dr. Ece Salihoğlu.

I would like to express my special thanks to Assoc. Prof. Dr. Ergin Koçyıldırım and Assoc. Prof. Dr. Ece Salihoğlu for very helpful discussions and endless support.

Furthermore, I would like to thank my colleagues, Innovative Polymer Nano-Therapeutics Research Group all members. Especially, I thank Erhan Demirel who helped me with his constant guidance, cooperation, and support.

I would like to thank Alper Savaş, Havva Mamedova, Samet Özer, Engin Sümer, Ekrem Musa Özdemir, Barış Cebeci and all MEDITAM employees who helped me in the background of this project. Also, thanks to TUBITAK for supporting our project.

My heartfelt thanks to my mom who means the world to me, for always supporting my dreams. My family is the pillar of my life, and I am forever grateful to them for showing faith in me and giving me the liberty to choose what I desired.

Finally, but definitely not the least, my special words of thanks should also go to my husband Mansur Akçay. His permanent love and confidence in me have encouraged me to go ahead in my studies and career. I am truly thankful for having you in my life. I consider myself the luckiest in the world to have such a supportive husband, standing behind me with his love and support.

Contents

List of Figures

List of Tables

Chapter 1

Motivation

Trauma is a life-threatening situation that is divided by blunt force trauma when the object hits the body, giving rise to deep cuts, concussions or broken bones and penetrating trauma when the object makes a hole the body creating an open wound. Hypovolemia is the state of reducing the blood volume of the body due to extreme bleeding more specifically after trauma [1]. Hypovolemic shock is also known as hemorrhagic shock. The hypovolemic shock that is resulting from abrupt and critical loss of circulating blood volume might cause sequentially to hemodynamic instability, diminishes in oxygen delivery, tissue perfusion and organ damage, then finally, it could result in death. Hemorrhagic shock is the most substantial death cause among traumatized patient serious hypovolemia depending hemorrhage is responsible for half of the traumatized death. Death happens within 2 hours after trauma.
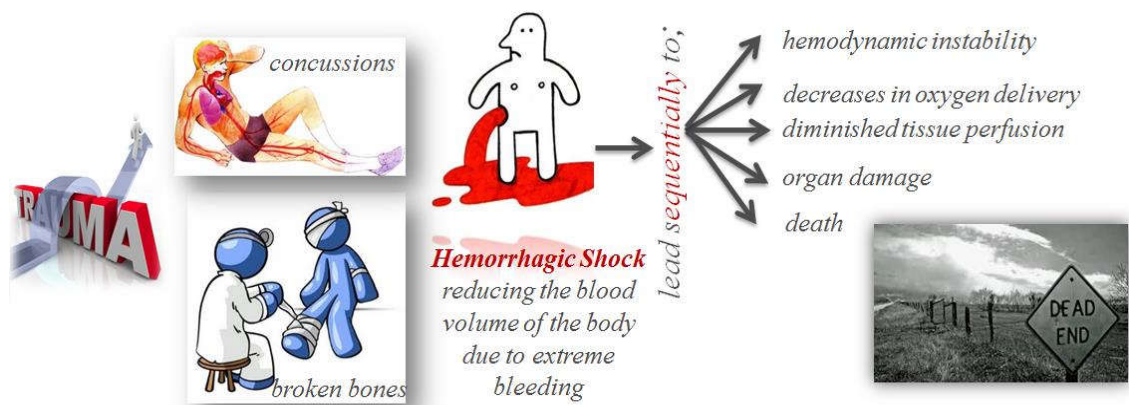
Figure 1.1: Hemorrhagic shock is the most substantial death reason among traumatized patient

The conventional approach for hemorrhagic shock depends on hemorrhage control and volume expansion is putting the lost volume back using crystalloids or colloidal liquids, transfusion of donor blood or using blood substitutes.

Unfortunately, the transfusion of blood has some disadvantages. The first thing is the lack of a donor. Blood type mismatch that can occur even if the donor is found. Another thing is that the cold chain must be protected while blood is being transported. Despite everything, most of the time, red blood cells lose their ability to carry oxygen after transfusion. The transfusion of stored red blood cells may often not much right solution to re-establish microcirculatory oxygenation.

Another strategy is putting the lost volume back by using colloids and crystalloids. That case requires intrinsically large volumes. Resuscitation in large volumes brings along detrimental side effects including coagulation disturbances and complications of gastrointestinal and cardiac [2]. On the other hand, just enough liquid should be given and never loading liquid to alter blood pressure back to the normal level, otherwise, hemorrhage will be increased and this increase may lead to mortality.

Because of this reason, there is an urgent need for aggressive resuscitation agents that can fix endogenic and hemostatic mechanism which are disturbed during hemorrhagic shock. In an ideal fluid resuscitation, solely small volumes should put back to handle the hemorrhagic shock [3]. Therefore, there is a need for resuscitation agents that will work even at small concentrations.

1.1 Fluid Resuscitation

Critically trauma patients lose large amounts of blood suddenly; in that case, they need additional fluids promptly to prevent dehydration or kidney failure. Besides the timing of volume replacement, the type of resuscitation fluid becomes important. Crystalloids and colloids are commonly used as resuscitation fluids in clinical. Crystalloids are solutions containing electrolyte and nonelectrolyte solutes that can pass freely through capillary membranes. Isotonic saline, Ringer's Lactate and Plasma-Lyte are most commonly used as crystalloids. Crystalloids have the primary effect on the interstitial and intracellular compartments. Colloids are high-molecular-weight substances to restrict passage across capillary membranes including dextran, hydroxyethyl starch (HES), albumin and gelatin. Colloids have the primary effect on the intravascular section [4]. Gosling in 1998 suggested that colloids such as HES since it has better retained in the vascular system rather than albumin and gelatins, it has a positive effect on the mortality. The same study was carried out among hypertonic crystalloids and

2

isotonic crystalloids. Hypertonic crystalloids have significantly decreased the death rate [5]. The SAFE Study Investigators in 2004 investigated the effects of albumin and saline. In the study, while albumin was applied to 3497 out of 6997 patients, saline was given to 3500 patients. When the number of deaths of these two groups was examined, the albumin group had 726 deaths and the saline group had 729 deaths. They showed there are no important differences between crystalloid and albumin-based treatments. This study also spoiled the belief that crystalloids in much more bigger volumes ought to be applied to reach the same resuscitation with very small colloidal fluid volumes. On the other hand, the colloids especially albumin because of being a blood product is higher cost than crystalloids. Another disadvantage of albumin due to be the blood product is to have the potential being infectious disease carrier [6].

1.2 Drag Reducing Polymers (DRP)

Drag reducing polymer (DRP) is a well-described hydrodynamic phenomenon observed in turbulent flow in a pipe and this is known as the Toms effect [7]. In 1948 B.A.Toms, in monochlorobenzene has shown that high molecular weight poly (methyl methacrylate) significantly reduces the resistance to turbulent flow in the hose. This knowledge has led many scientists to understand the mechanism of the event and to use it for different purposes and applications. The idea is contemplated that water-soluble polymers can be used in bio-systems by demonstrating that poly (ethylene oxide) (PEO) [8], poly(acrylamide) (PAM) [9] and natural polysaccharides also in the same manner reduce resistance to turbulent flow in the hose [10]. In fact, these polymers have no effect on the resistance of the linear flow in a pipe, but have the effect of reducing the hydrodynamic resistance in the defective laminar flow, which is not considered to be a complete turbulence, or in the pulsed flow in the flat and spiral pipes [8][11]. The working mechanisms of DRP are still not fully elucidated. The first use is to save cost and energy by maintaining the pressure drop due to turbulent flow in petroleum pipelines, thus achieving petroleum pumping at lower pressure. Albeit the open mechanism is not known, the pressure of the petroleum to the wall of the pipeline is responded in the same way and this interaction creates turbulent flow. As for drag reducing agents, they act as turbulence breaker by interacting with both petroleum and wall (Figure 1.2.1).

For years, research has been carried out on this subject and it has been aimed to expand and improve the use of DRP in the industry. However, the greatest limitation of DRP's use in industry [12][13] is that they are mechanically degraded due to the high shear force they are exposed to. Many organic or water-soluble derivatives have been found after the discovery of DRP. At low concentrations, these long polymer chains can reduce the flow resistance by up to 80% [10]. In order to have drag reducing effect, it is required high molecular weight and linear structure. The abilities of drag reduction depend on the degree of polymerization (number of repeating monomers along the chain) and the size of monomer. From the two DRPs of the same molecular weight, the one has smaller molecular weight of monomer shows stronger drag reducing [14]. The DRPs are not effective in laminar flow. However, DRPs can decrease resistance in non-turbulent flow, like vibrating flow in the smooth line, eddies at low Reynolds numbers. DRPs are composed of different types of polymers; organic polymers such as polymethylmethacrylate (PMMA), polystyrene; synthetic DRPs like PEO, PAM and natural polymers like hyaluronic acid, carboxymethylcellulose, several bacterial polysaccharides. Recently, a new type of DRP was explored that is extracted from the aloe-vera plant. In 2002, Kameneva et al. investigated the newest DRP isolated from the essence of aloe-vera leaves in terms of their chemical, rheological and hydrodynamic properties [15]. This aloe-vera based DRP has been used as a resuscitation agent in fatal hemorrhagic shock-induced animal models and significantly increased survival. In addition, this DRP was also studied in the acute myocardial ischemia model and significantly reduced deaths. Figure 1.2.2 shows that the aloe-vera plant and the gel extract from the inside of its leaves [16]. This polymer has proven to be the most potent and effective DRP compared to PEO, PAM and PNVF.
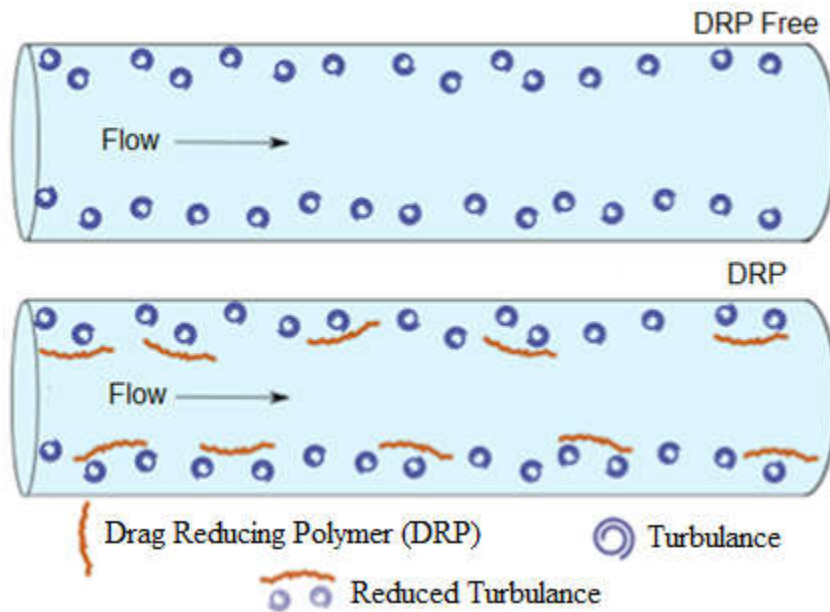
Figure 1.2.1: The turbulence effect by DRP

Figure 1.2.2: Aloe-vera gel extraction from aloe-vera plant

The effects of DRP on in-vivo blood circulation have been studied in many studies since the 1970s. The first study tests that polymers with a linear long chain and a molecular weight greater than 10^6 can reduce turbulence friction as a blood transfusion fluid [12]. Subsequently, another group demonstrated the effect of PAM on the turbulent flow of cow blood in a glass tube [17]. Again by the same group, the percussive flow effect of DRP in turbulent and linear flow was demonstrated by the experiment on the puppy that DRP significantly reduces flow disorders after arterial occlusion [16]. Some concurrent studies are; DRP reduces blood pressure in normal and hypertensive rats, and while the blood flow was increased to the carotid artery without a change in arterial pressure in dogs, animals with DRP injection for 6-8 months had lower blood pressure without any

toxic effect. In addition to intravenous injection, oral DRP loading has been shown to have no effect, even with a high dose [15]. Gregorian et al. observed a spontaneous decrease in arterial blood pressure and an increase in blood flow towards the carotid artery in the study injected DRP into dogs. In another model in rabbits, DRP has been shown to increase the number of functional capillaries in the damaged areas caused by ischemia [15]. The use of DRP as a resuscitation agent has been extensively studied by the group who explore the natural and effective DRP at the University of Pittsburgh. To increase tissue perfusion without an increment in arterial blood pressure is very important for resuscitation after a severe bleeding, because increased blood pressure is known to cause secondary bleeding. Kameneva et al. suggested that soluble DRP may be added to the resuscitation fluid, and they resuscitated by using PEO, hyaluronic acid and aloe-vera based DRP in the isotonic solution to the animals under hemorrhagic shock [7][3][18][19][20]. These blood-soluble polymers have been shown to inhibit death resulted from hemorrhagic shock. In the study performed in rats, the activity of PEG weighing 3500 kDa and aloe-vera extract DRP was compared with low molecular weight PEG (200 kDa) and 2.4% dextran. The results showed that DRP solutions significantly increase tissue perfusion and oxygenation. In addition, survival in the 2-hour period after hemorrhage increased by 100% for both DRPs, while increased by 14% and 19% for PEG (200 kDa) and dextran. The results showed that in addition to be used as a resuscitation agent, the weight of the polymer (degree of polymerization) is also important in order to be an effective DRP. PEG (200 kDa) did not show efficacy as DRP even at a higher dose (by 1.5 times) and higher volume (by 3 times). Another study by the same group showed that survival times were prolonged in rats treated with aloe-vera-based DRP as a resuscitation agent. When animals losing 52% of the total blood volume were given an isotonic solution containing 50 ppm of DRP in 12% of their total blood volume, the survival rate increased by 33%, and this rate was only 7% in the control experiment [18].

According to Tom's effect, DRP works very well turbulence in the pipeline, but in the human vascular system, there is no turbulent flow. However, turbulent flow can be mentioned in aorta, flow separation and bifurcations. That's why in our project, we are aiming to investigate how DRP works in the circulatory system.

1.3 How DRP works in vascular system

Although there is a lot of study in the industry with DRPs, their biomedical applications have not still known very well. Nowadays, it has been investigated that this polymer has the ability to decrease vascular resistance to turbulent flow even adding at very small concentrations into the blood circulation [3][18]. In here, besides reducing the resistance of the turbulence flow, it is shown that enhancing blood flow, tissue perfusion, and oxygenation without changing blood viscosity in the circulation. With this study, the idea that DRP can be used as a resuscitation agent has emerged.

On the other hand, traditional fluid resuscitation has limitation due to requiring administration of large volumes of fluids that are intrinsically heavy and bulky. Studies showed that an enough volume of fluid should be given to avoid death from deep hypotension after severe blood loss but without blood pressure normalization otherwise, hemorrhage will be increase and this increment may lead mortality [7]. In this context, an ideal initial resuscitation fluid for the overcome of hemorrhagic shock would require management of solely a small volume to evolve tissue perfusion and oxygen utilization without increasing blood pressure to such an extent that endogenous hemostatic mechanisms (soft platelet-fibrin plugs) are disrupted [18]. Because of this reason, there is an urgent need to aggressive resuscitation agents that can fix endogenic and hemostatic mechanism which are disturbed during hemorrhagic shock. Drug reducing polymers (DRP) have significant effect on blood circulation even if it is added very small concentration into blood. With the discovery of the presence of water-soluble DRP, it is thought that the blood flow in the vessels will have an effect as in the pipelines. Turbulent flow in petroleum pipelines is not expected in the main and capillaries in our circulatory system (Re <1000 according to the Reynolds number), but rather a linear flow is observed. Therefore, the pressure balancing of the DRP by acting as a turbulence breaker in the turbulent flow does not apply to the circulatory system. In fact, scientists from different disciplines who conducted in-vitro and in-vivo studies on the effects of DRP on blood circulation were not initially aware of the Reynolds number. The Reynolds number of the cardiovascular system was too small for the DRP to create Toms' effect in a small experimental animal [16][21]. Thus, the working mechanisms of DRP in the circulatory system should be different, and further research was carried out in this direction. Preliminary in-vivo studies were that the observed effect was not related to the change in the viscosity of the blood. Although they had

different chemical structure (PEO, PAM, polysaccharide), they showed the same hemodynamic effect when injected in nano-concentration. The common feature of all is to reduce the resistance to turbulent flow. On the other hand, PEG which has a molecular weight of 200 kDa, did not show a drag-reducing effect even if it is injected at a 15-fold high concentration compared to PEG with a molecular weight which is greater than 1000 kDa. Coleman et al. had previously observed that showed no efficacy compared to the mechanically degraded DRP (e.g. Separan A-273) not degrading analogue [22]. At first glance, these data indicate that the activities of DRP are primarily dependent on physical properties. Injection of synthetic or natural DRP into the bloodstream at a very low concentration, decreasing blood pressure in normal or pathological tissues, increased capillary density in diabetes animals, increased survival in myocardial perfusion and myocardial infarction, a significant increase in survival time after deadly hemorrhagic shock many small and large scale improvements have been observed [7][23]. In some studies, it has been shown that DRP in the high concentration of intravenous administration for a certain period of time inhibits vascular occlusion of animals in the high cholesterol diet. Even though there is no clinical study of DRP yet, many studies on the positive effects on blood circulation are to predicted to develop DRP from the laboratory to the patient [24][25]. Another hypothesis is that the DRP reduces the loss of pressure from the artery to vein. Pacella et al. has examined this hypothesis by measuring the pressure difference in the arteries and veins before and after DRP injection [23]. DRP supplies greater capillary pressure by decreasing loss of pressure from artery through vein. The pressure decreases during blood circulation in the body naturally. Another explanation is that DRP does the blood can reach the capillary vessels with a higher driving force by reducing the pressure loss and hydraulic energy loss. They help the blood reach the smallest capillaries at a certain flow rate. In addition to vessel geometry and blood viscosity, they also contribute significantly to vortices in flow separation and bifurcation. The effect of DRP on flow separation is shown in the vessel bifurcation model in vitro. As previously mentioned, the effects of flow separations at the bifurcation points of the DRP have been investigated.
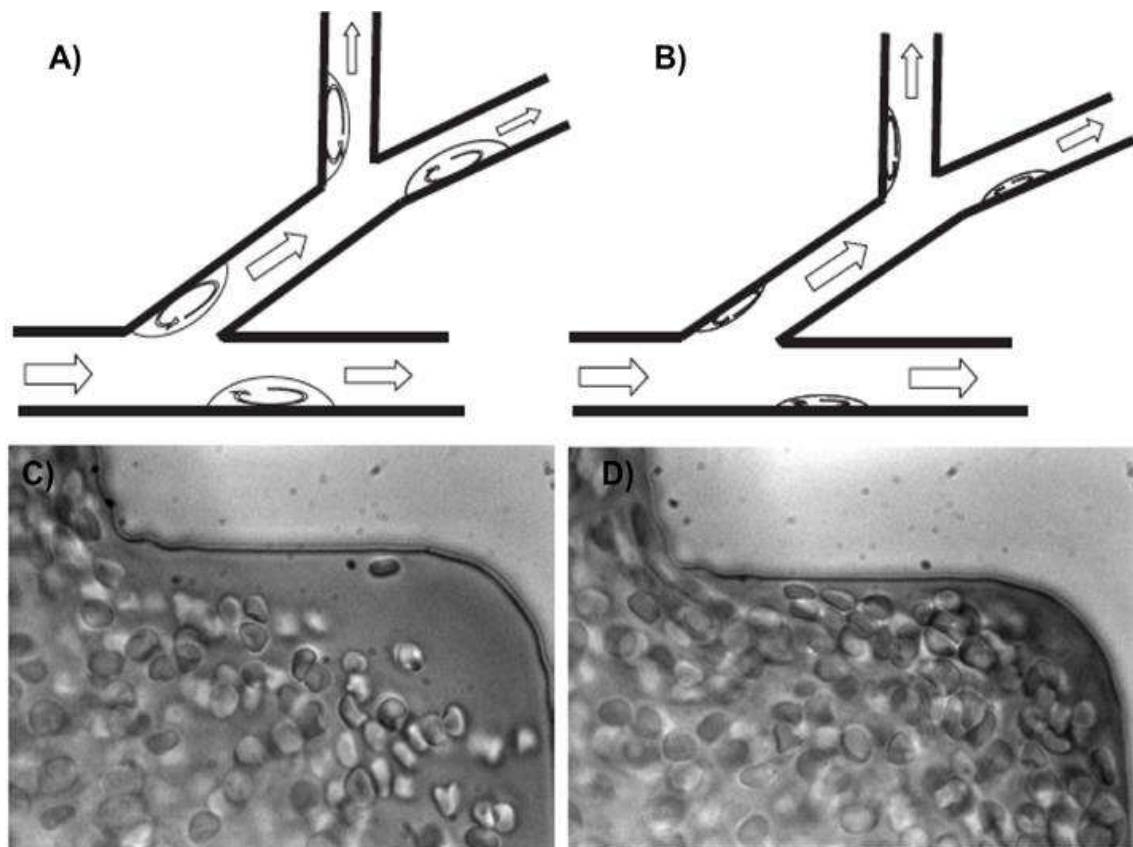
Figure 1.3.1: DRP's effect on flow separation and vascular bifurcation A) Flow separation with DRP-free, B) Flow separation with DRP (PEO, 10 ppm), C) vascular bifurcation with DRP-free blood, D) vascular bifurcation with DRP-containing blood.

Experiment has done by measuring flow-velocity profile near the bifurcation with a low Reynolds number model. In this research, it was observed that DRP diminishes the turbulence in flow separation and, by this means DRP retards to be swirl in the bifurcations (Figure 1.3.1 A and B) [16]. This effect reduces the pressure loss in the artery, thereby increasing the pre-capillary pressure, functional capillary density and tissue perfusion, and eliminating the blood circulation in the capillary vessels caused by hemorrhagic shock. Approximately 20 years later, the DRP effect on the separation of blood flow, which brings out very important data, is explained by using expandable micro channels [26]. In the control experiments which no DRP was given, large flow separations were observed in expansions due to decellular areas near the canal wall. After the addition of DRP (10 ppm), the flow of red blood cells (RBC) was rearranged and they were directed towards areas near the wall where the plasma was intense (Figure 1.3.1 C and D). Thus, DRP implicate in the flow cycle again the flow at the expansions by reducing or eliminating the flow separation. According to the Fahraeus-Lindquist effect, cell-free areas are located near the walls of veins smaller than 0.3 mm

[27]. Cotoia et al. in 2009, were used Hyaluronic acid and PEO as DRP and, they showed in the animals which losing 4% of the total body blood, the survival time was increased after hemorrhagic shock. While all of the control group animals of this experiment died, the survival rate within 3 hours following the bleeding increased by 50% in DRP treated animals [7]. In the light of these data, in contrast to the intervention of the DRP to replace lost volume in cases of severe injuries and serious blood loss, DRP solutions to be given in small volumes can be increased the survival rate in 3 hours after major trauma. When the volume transformation in this rat study is adapted to an adult human, DRP can be applied as a promising approach in a small volume of 200 mL, an alternative to classical methods. In the light of these applications, it is clear that cardiovascular diseases, hypertension, diabetic microangiopathy, atherosclerosis; tissue ischemia caused by vascular occlusion can be treated or prevented by intravenous DRP injection. The effects of DRP on blood circulation also shed light on other potential treatments. For example, DRP allows the red blood cells to mix with the site where the placement is located in the dense area prevents the migration of platelets to this area, which may prevent the clotting problem and leukocytes from shifting into this area. Thus, inflammation can be reduced [28]. In this way, the effect of regular intravenous DRP injection on the biomaterial implanted animal, whether the body reacts to the implant, affects the biodegradation, and tissue growth on the implant was investigated. After a porous biomaterial, which was naturally degraded by microphages, was placed in 3 groups of rats (PEO, aloe-vera based and control group), animals were injected with DRP twice a week (0.3-0.4 nM). The control group was an isotonic solution and after 7 weeks there was no difference in the weight and behavior of the animals compared to the control group. In the histological analysis, it was observed that the implants in the control group completely degraded, whereas a significant portion of the implant remained intact in the DRP injected groups. These results indicate that DRP reduces inflammation reactions by regulating red blood cell and leukocyte traffic in the vessel wall [29].

1.4 Oxygen Carrying Mechanism of DRP

DRP increases the number of red blood cells near the blood vessel wall (hematocrit) [30]. This can also be used to explain the DRP's oxygen transport mechanism. DRP activates oxygen transport, allowing red blood cells to be closer to the tissue. But the regions, where the density of plasma already reduced via DRP, will be more effective in

the transfer of oxygen anymore? Kameneva et al. also suggested in addition to blood pressure, O_2 consumption and CO_2 production in the body were measured, and O_2 consumption and CO_2 production increased in DRP treated animals [18]. DRP has also been shown to reduce oxygen deficiency in the liver after hemorrhagic shock. Another point that Kameneva and her friends elaborate was whether DRP could be the solution to the oxygen deficiency (hypoxia) in the liver cells after hemorrhagic shock. In the experiments performed for this purpose, a controlled bleeding, 30 minutes after 1000 kDa molecular weight PEG and isotonic solution as control was given, was carried out at a constant pressure (MAP 40 mmHg). At this point, 1 mL of DRP and control is given to the animal as a second dose. Immediately thereafter, an immunofluorescence dye called EF_5 was injected into the vein, and liver cells without oxygen (hypoxic) were stained to red. While the results showed that most of the liver cells were hypoxic in the control group, it was seen that very few cells remained oxygen free in the DRP injected group [20]. The effect of DRP on tissue oxygenation contributed to the direction of future studies.

1.4.1 Oxygen Carriers: Hemoglobin Derivatives and Perfluorocarbon (PFC) Derivatives

Oxygen carriers are solutions that have the capability to transport oxygen and are developed as red cell substitutes able to increase the oxygen-carrying capacity of the blood [31][32]. They are classified as hemoglobin derivatives and PFC derivatives. They use different mechanisms to carrier oxygen. While hemoglobin binds to oxygen chemically, PFCs have the ability to physically dissolving significant quantities of oxygen.

Hemoglobin is a protein found in red blood cells made of four subunits in which there are two alpha and two beta subunits and each of them encircles a central heme group which rich in iron attached to each subunit. Iron gives the blood the red color. Each subunit binds one oxygen molecule, allowing each hemoglobin molecule to bind four oxygen molecules. Iron ion chemically reacts with oxygen. Molecular oxygen binds to the iron center of the hemoglobin that leads to releasing of protons from the acid units which decrease the pH. Low pH provides conversion of Fe_{III} to Fe_{II} and the releasing of oxygen to tissues [33].

Perfluorocarbons (PFCs) are synthetic molecules that have the carbon backbone that is substituted with fluorine atoms. They are chemically inert because of the highly powerful chemical bonds between fluorine and carbon atoms. Additionally, they are able to physically dissolve significant quantities of most gases including oxygen, carbon monoxide (CO) and carbon dioxide (CO_2). Perfluorocarbons carry out the passive transportation of gases dissolved, in direct proportion to their partial pressure. PFCs in the circulation are just like increasing the solubility of oxygen in the blood plasma. Oxygen releasing by PFCs is not depending on pH. There is no oxidation or other modification over time in PFCs. Their oxygen delivery and releasement are not influenced during circulation. They occupy inter RBC spaces and the plasma layer. Accumulated oxygen in here makes easy to the diffusion of oxygen to the tissue.

In this study, the drag-reducing polymer (DRP) extracted from the aloe-vera plant mainly during hemorrhagic shock was used as a resuscitation agent. DRP has a positive effect on tissue perfusion. To contribute to the oxygen-carrying ability, PFC derivatives were preferred because of the difficulties of mimicking hemoglobin systems. DRP was modified by the PFC group which allows more oxygen to dissolve in the blood and the effect of tissue perfusion was strengthened.

1.5 Hemorrhagic Shock Model in Animals

Hemorrhagic shock is a physiological condition. Depending on severe blood loss, tissue perfusion diminishes, cellular hypoxia, and metabolic damage happens in the circulatory system [30]. Pre-clinical studies should be applicable as clinically. To make physiological mechanisms and immunological responses based on deep hemorrhage more understandable requires animal models. Until now, almost everything that we know about hemorrhagic shock comes from animal studies. For years, hemorrhagic shock models were developed to explain pathophysiological mechanisms of shock and to estimate efficacies of therapeutics. However, there is still a need to create models closer to human beings [34].

The most important things to generate an ideal animal model are to perform easily and to be able to mimic closely human anatomy and physiology. For investigating the pathogenic mechanisms of severe bleeding primarily used small animals, while the examination of treatment strategies to use large animals is more appropriate. Because of being cheap and easy to access, mice are more preferred. However, their small size and being a low volume of blood are disadvantages. When the rats and rabbits compared

with mice, their larger body size and blood volume make them more easily applicable to the hemorrhagic shock studies.

In hemorrhagic shock studies, it is very difficult to simulate the condition of shock and to achieve standardization in the clinical setting. There are three models commonly used in hemorrhagic shock studies as fixed-volume hemorrhage, fixed-pressure hemorrhage, and uncontrolled hemorrhage. In fixed-volume hemorrhage model, a certain percentage of the calculated blood volume based on body weight was calculated. The calculated amount of blood was withdrawn. The main advantage is that it allows investigating hemodynamic response and compensation mechanisms of the animal`s body. But, experimental standardization and repeatability are difficult. In fixed-pressure hemorrhagic shock model, bleeding is carried out until a certain arterial pressure which is predetermined and arterial pressure provided to be stable at this point. The fixed-pressure shock model allows being checked the degree and duration of hypotension by the following of blood pressure. Thus, standardizations and reproducibility are more reliable under hemorrhagic shock condition. Due to this, this method commonly used for the evaluation of physiological alterations and organ damages. Although fixed-volume and fixed-pressure models promise to keep under control severe bleeding, these models cannot emulate the situation after vascular trauma resulting from artery injury and interior organ injuries. Therefore, the uncontrolled hemorrhagic shock model is used to mimic keep under control free bleeding from aorta disruption [30][34].

Until now, aloe-vera based drag-reducing polymers were worked on rats. Working on rabbits rather than rats was preferred because they had more weight and blood volume and had not been studied before. On the other hand, the hemorrhagic shock was performed until the mean arterial pressure (MAP) decreased to a predetermined constant pressure which is called a fixed-pressure model. The most important advantage of this was able to follow the MAP in a controlled manner.

Chapter 2

Experimental Section

2.1 Materials

Aloe-vera plant (Fidan Istanbul, Yalova/Turkey), PEG (4500 kDa, Dow Chemical), N,N-dimethylformamide anhydrous (DMF, Sigma- Aldrich, 99.8%), pentafluoro-propionic acid (Sigma-Aldrich, 97%), heptafluoro-butyric acid (Sigma-Aldrich, 99%), perfluoro-pentanoic acid (Sigma-Aldrich, 97%), undecafluoro-hexanoic acid (Sigma-Aldrich, 97%), N-(3 dimethylamino-propyl)-N'- ethylcarbodiimide hydrochloride (EDC, Sigma-Aldrich, 98%), 4-dimetilaminopiridin (DMAP, BRAND), N,N-dimethylformamide anhydrous (DMF, Alfa Aesar, 99.8%), dialysis tubing cellulose membrane (MWCO=50,000 Da, Spektra/Por®7), triton-X 100 (Biomatik), phosphate buffer solution (PBS, Multicell, Wisent Inc.), ethanol (Sigma Aldrich, 99.8%), Ringer's lactate solution (Free Flex), 0.9 isotonic saline solution (Free Flex), catheter (Neocan™), xylazine (Rompun®, %2), ketamine (VetaKetam®).

2.2 Characterisation

To confirm of the synthesis of the AVDRP and AVDRP/F Agilent VNMRS 500 MHz nuclear magnetic resonance spectrometer was used to carry out the Hydrogen nuclear magnetic spectroscopy (^{1}H-NMR) and Fluorine nuclear magnetic resonance spectroscopy (^{19}F-NMR). AVDRP and AVDRP/F were inspected, and the results were compared. A Fourier transform infrared spectroscopy (FTIR) was carried out using the FTIR spectrometer (Spectrum Two N™, Perkin Elmer). FTIR of AVDRP, AVDRP/F were performed using a diamond crystal, with range of 4000 cm^{-1} to 400 cm^{-1}, resolution of 4 cm^{-1}, and 16 scans per minute. The peak shifts were observed and compared to each other to confirm the synthesis of the polymers. Investigation of the molecular weights of the AVDRP and AVDRP/F was performed by Gel Permeation Chromatography with dynamic light scattering detector (Ecosec GPC/SEC System,

Tosoh Bioscience). To see and compare the weight loss profiles of AVDRP, AVDRP/F, they were tested through thermal gravimetric analysis (TGA) using TGA 8000 Perkin Elmer. The weight loss was measured as a function of temperature. The heat flow was 10°C/min, from 25°C - 600°C, under nitrogen flow. The results were compared to see the degradation/stability of each polymer. To analyze the textural changes on the samples and how they differ from each other at nano level, AVDRP, AVDRP/F and PEG were imaged in a scanning electron microscope (SEM, Philips XL 30S FEG with EDAX detector). The samples were also checked for % fluorine, carbon and oxygen contents using the Energy dispersive x-ray spectroscopy (EDAX) detector in the SEM. The rheological measurements were performed at 37°C by using a modular compact rheometer MCR 102 (Anton-Paar). Shear stress was followed between the ranges 10^{-1} - 10^{-2}, while shear strain measurements were carried out in the strain range of 10^{0} - 10^{2} % at a frequency of 2 Hz. In viscosity measurements, the shear rate was decreased from 10^{2} to 10^{0} s^{-1}. Blood samples were from the central ear artery of the rabbit into heparinized blood tubes and were renewed every two hours to minimize blood clotting. They were kept at +4 until use. For each sample prepared at different concentrations respectively 10, 20, 50 ppm. 900 µl blood were used and saline was added into 10, 20 and 50 ppm of solution. After mix, 750 µl solution each one of them respectively was placed into plate. Rheological properties such as viscosity, loss modulus, storage modulus vs. shear rates and shear strain were analyzed. Additionally, the viscosities of the polymers were also investigated with Brookfield DV2T Viscometer. In vivo studies were approved by the Istanbul Medipol University Ethics Committee in Animal Experimentation. Male and female New Zealand rabbits (n=4, 2 to 3kg) were obtained from Istanbul Medipol University Medical Research Center (MEDITAM, Turkey). All animals were acclimated for 2 weeks before the experiment. All animals were treated in accordance with animal welfare.

2.3 Extraction of Drag Reducing Polymer

In the first step, drag reducing polymers were extracted from aloe-vera plant. Aloe leaves were cut at the bottom and extensively washed. Gel in aloe-vera leaves were peeled and pulp was collected. The mass of the gel was weighted and added deionized water (Direct-Q 3 Ultrapure Water System, LabRepCo) (1:0.5 v/v). Gel mixture was shaken by overhead stirrer (Wise Stirr HA-120) vigorously at 50°C for 2 h to make more soluble extract. Then, mixture were continued to shake at room temperature for

overnight to homogenize completely. Homogenized gel was centrifuged at 10000 rpm for 20 min at 4°C. After centrifugation, to remove water from the gel vacuum distillation was performed at 45°C, 100 mbar. After distillation was completed, concentrated gel mixture was dialyzed against DI water using a 50 kDa molecular weight cutoff cellulose membrane (Spectra/Por® 7 Pre-treated Standard RC Dialysis Tubing) for 48 hours by replacing the water frequently. The final dialyzed product was dried using freeze dryer (CHRIST ALPHA 1-2 LDplus Freeze Dryer) then powder was obtained. Dried powder was stored under dry conditions at +4°C until use.
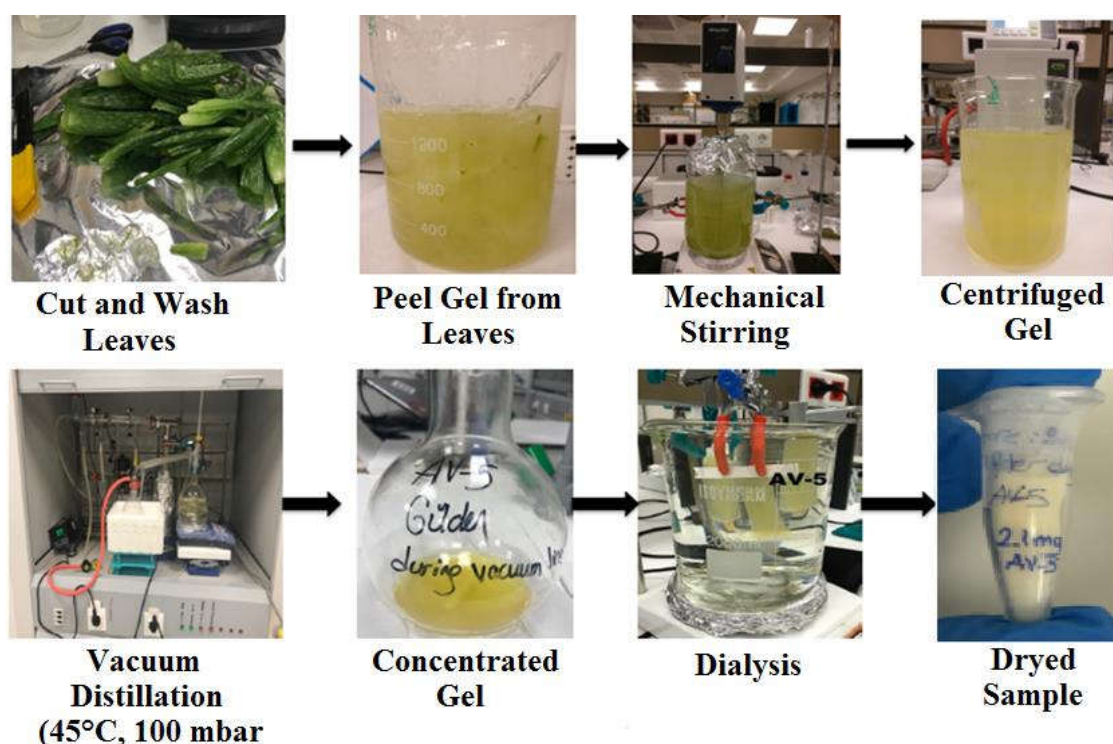
Figure 2.3.1: Extraction of aloe-vera gel

2.4 Sytnhesis of Fluorinated Drag Reducing Polymer

Drag reducing polymer which is extracted from aloe-vera plant was modified with perfluorocarbons to be able to enhance oxygen carrying property. 50 mg AVDRP for each perfluorocarbon group was dissolved in 40 ml anhydrous DMF to be clear solution. After solubilization, pentafluoro-propionic acid was calculated as 2.5% by weight of the AVDRP polymer. Then, pentafluoro-propionic acid, EDC and DMAP were mixed at 1:2:1 ratio. Afterwards, the solution which contains AVDRP and DMF was added drop by drop into acid, EDC and DMAP mixture under the nitrogen gas and stirred at 700 rpm, overnight. Next day, 20 ml deionized water was added and then keep stirring one more hour. Final step was dialysis for purification of fluorinated DRP

solution. Fluorinated DRP (AVDRP/F) solution was dialyzed against DI water using a 50 kDa molecular weight cutoff cellulose membrane for 48 hours. Following dialysis, the solution was shell frozen in liquid nitrogen and freeze dried. The lyophilized powder stored under dry conditions at 4°C until use. All these procedures were repeated for heptafluoro-butyric acid, perfluoro-pentanoic acid, and undecafluoro-hexanoic acid respectively.

Although the clear structure of aloe-vera gel is not known, its structure has been tried to be determined in some studies. In one study, the polysaccharide structures in the aloe-vera gel have been described four different linear glucomannans with partially acetylated which includes 1-4 glycosidic linkages [35]. In another study, Chow et al. proposed the main component of aloe-vera gel structure depending on data compositional analysis of carbohydrate, chromatography, and NMR. The structure is composed of a linear mannose backbone with β-1,4-linked glucose [36]. Based on all these assumptions, we aimed to conjugate the aloe-vera including OH groups with perfluorocarbons to increase tissue oxygenation and tissue perfusion.
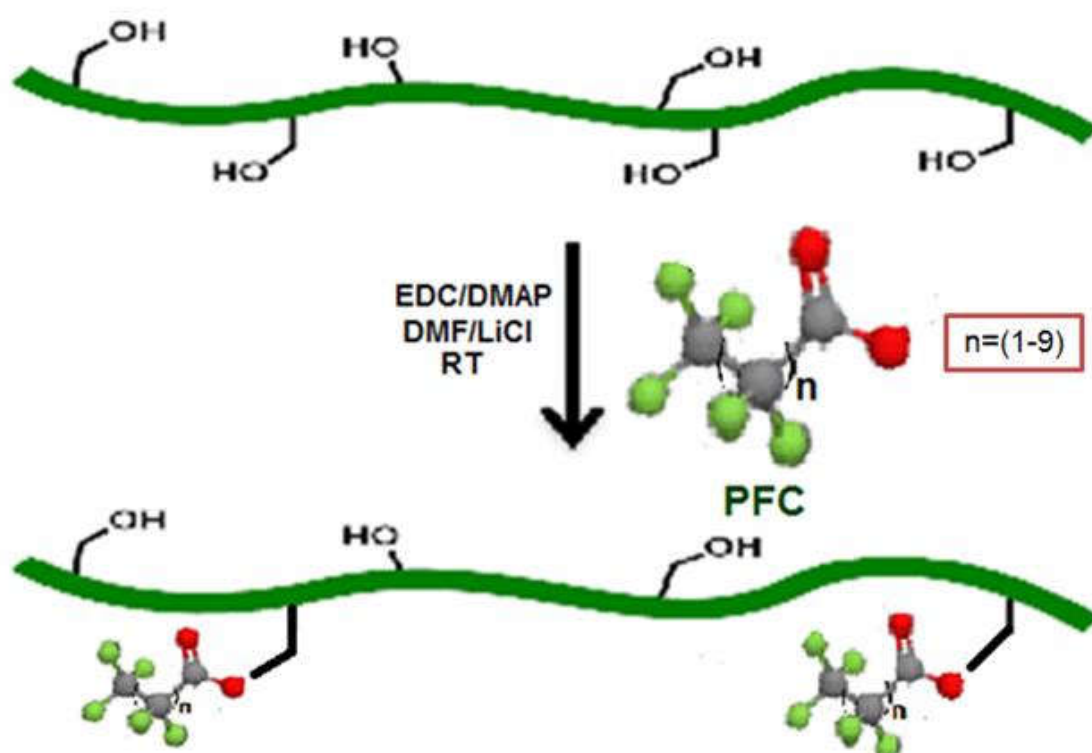
Figure 2.4.1: Fluorinated aloe-vera extracted long chain polysaccharide

2.5 Determination of Drag Reducing Ability

Since Reynolds numbers are small depending on the vessel diameter, there is no turbulent flow in the circulatory system. Nevertheless, it is known in the literature that DRPs work effectively in a turbulent flow. Therefore, drag reducing effect (DRE) of AVDRP and PEG was investigated in the generated flow system by placing pressure probes at certain points on the ECMO (Extracorporeal Membrane Oxygenation) device as schematized in Figure 2.5.1. In this system, two types of the tube as 1/4" and 3/8" were used for creating turbulent flow. Reynolds number (Re) is used to determine the fluid's behavior. The turbulence flow occurs when the Reynolds number is above 4000. If the Re value is below 4000, either transition flow or linear flow occurs. In each tube, there is a distance at which the current stabilizes itself and no longer changes. This is known as the entrance length (Le). Pressure changes of the AVDRPs were measured by probes placed at these points to ensure that the current is of a constant type. Re value was calculated for AVDRPs at concentrations of 1, 10, 50, 100 ppm, respectively by the equation: $Re = 4Q/\pi Dv$ (Q: flow rate, D: diameter of the pipe, v: dynamic viscosity). The flow rate and diameter of pipe are known values for the system, but the dynamic viscosity was calculated from the kinematic viscosity measured by viscometer for each AVDRP and PEG concentration [dynamic viscosity = kinematic viscosity x density of the solutions]. The density of the solutions was determined by weighing the known volumes with precision scales (three repetitive measurements). The dynamic viscosity, Re and Le values calculated for the different concentrations in Table 2.5.1 and Table 2.5.2.
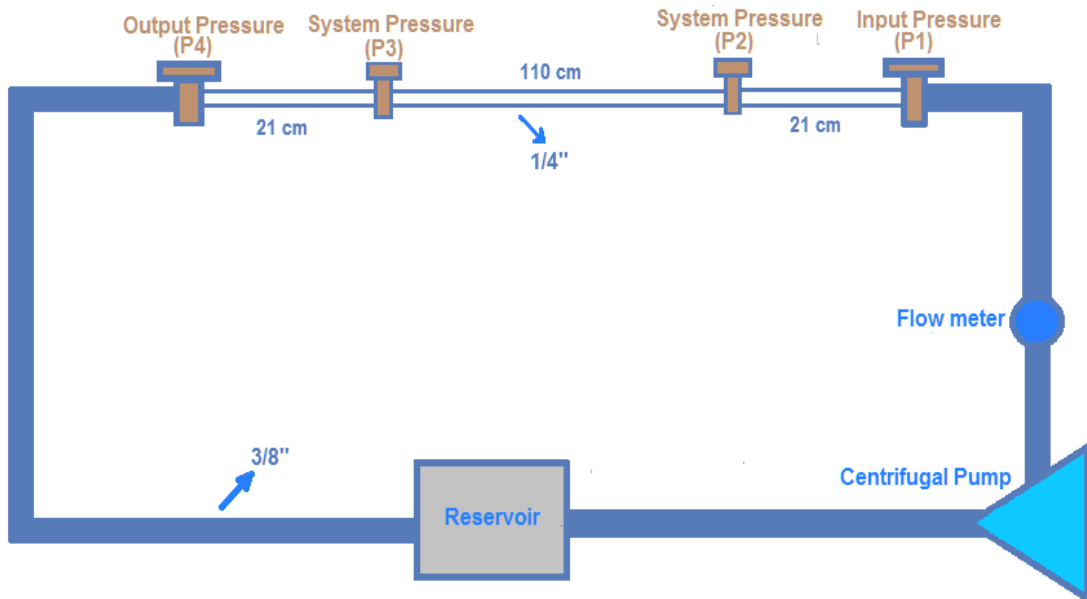
Figure 2.5.1: Schematic representation of ECMO

Table 2.5.1: AVDRP dynamic viscosity, Re and Le values at different concentrations and flow rates.

| Conc. (ppm)	Flow Speed (L/min)	Dynamic Viscosity (mm²/s)	3/8" Tube Re Value Re=4Q/πDv	1/4" Tube Re Value Re=4Q/πDv	3/8" Tube L_e Value Le/D=$4.4Re^{1/6}$	1/4" Tube L_e Value Le/D= $4.4Re^{1/6}$
100	1	0.99	2250.395	3375.593	~~	~~
	2		4500.79	6751.185	17.02	12.14
	3		6751.184	10126.78	18.21	12.99
	4		9001.579	13502.37	19.11	13.63
	5		11251.97	16877.96	19.83	14.15
	6		13502.37	20253.55	20.45	14.58
50	1	0.95	2345.149	3517.723	~~	~~
	2		4690.297	7035.446	17.14	12.23
	3		7035.444	10553.17	18.34	13.08
	4		9380.593	14070.89	19.24	13.72
	5		11725.74	17588.61	19.97	14.24
	6		14070.89	21106.33	20.59	14.68
10	1	0.98	2273.358	3410.037	~~	~~
	2		4546.717	6820.075	17.05	12.16
	3		6820.074	10230.11	18.25	13.01
	4		9093.432	13640.15	19.14	13.65
	5		11366.79	17050.18	19.87	14.17
	6		13640.15	20460.22	20.48	14.61
1	1	0.91	2448.232	3672.348	~~	10.97
	2		4896.464	7344.696	17.27	12.31
	3		7344.695	11017.04	18.47	13.17
	4		9792.927	14689.39	19.38	13.82
	5		12241.16	18361.74	20.11	14.35
	6		14689.39	22034.08	20.74	14.79

Table 2.5.2: PEG dynamic viscosity, Re and Le values at different concentrations and flow rates.

Conc. (ppm)	Flow Speed (L/min)	Dynamic Viscosity (mm²/s)	3/8" Tube Re Value Re=4Q/πDv	1/4" Tube Re Value Re=4Q/πDv	3/8" Tube L_e Value Le/D= $4.4Re^{1/6}$	1/4" Tube L_e Value Le/D= $4.4Re^{1/6}$
100	1	0.97	2296.79	2296.79	~~	~~
	2		4593.59	4593.59	17.09	12.19
	3		6890.38	6890.38	18.28	13.05
	4		9187.17	9187.17	19.18	13.68
	5		11483.97	11483.97	19.91	14.19
	6		13780.77	13780.77	20.52	14.63
50	1	0.94	2370.09	3555.14	~~	~~
	2		4740.19	7110.29	17.17	12.25
	3		7110.29	10665.43	18.37	13.10
	4		9480.38	14220.58	19.28	13.75
	5		11850.48	17775.72	20.62	14.27
	6		14220.58	21330.87	~~	14.71
10	1	0.95	2345.14	3517.72	~~	~~
	2		4690.29	7035.44	17.14	12.23
	3		7035.44	10553.17	18.34	13.08
	4		9380.59	14070.89	19.24	13.72
	5		11725.74	17588.61	19.97	14.24
	6		14070.89	21106.33	20.59	14.68
1	1	0.90	2475.43	3713.15	~~	10.99
	2		4950.86	7426.30	17.30	12.34
	3		7426.30	11139.45	18.51	13.20
	4		9901.73	14852.61	19.42	13.85
	5		12377.17	18565.76	20.15	14.37
	6		14852.6	22278.91	20.77	14.82

In this system, the largest Reynolds number we could reach was 14852 at 4L/min. Therefore, we have increased the Reynolds number to observe how the material will behave in the face of larger turbulence. For this, we changed the 1/4" tube diameter to 1/16". And a new Reynolds number was calculated for modified ECMO system (shown in Figure 2.5.2).
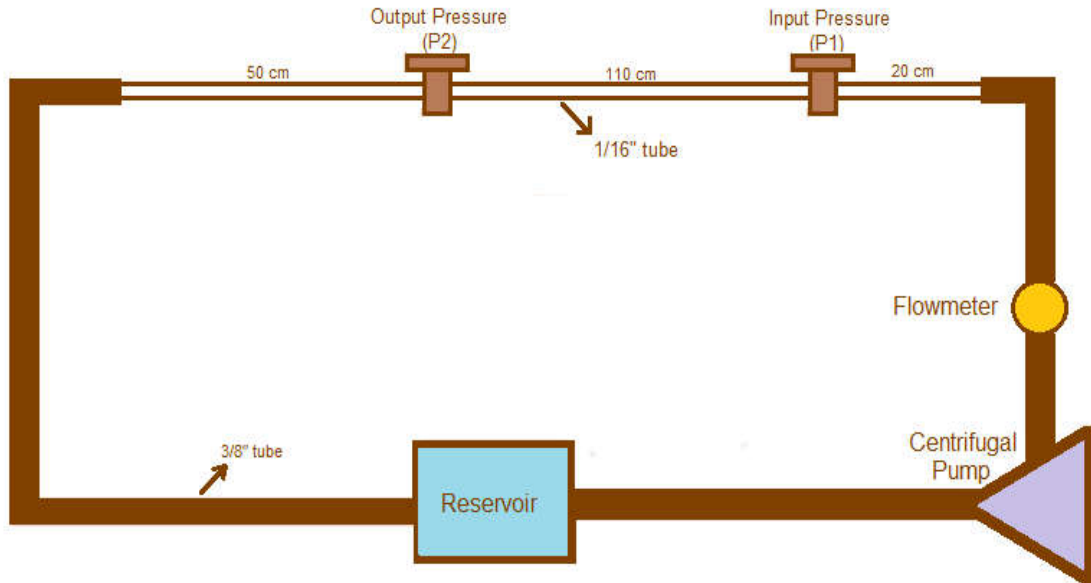
Figure 2.5.2: Schematic representation of the modified ECMO system

The Re (Reynolds number) and Le (entrance length) values calculated for this system are given in the following tables. Although the Le value was much shorter, a pressure probe was placed 20 cm later to ensure compatibility with the previous system. Because the type of flow after Le is constant throughout the tube. The pressure value of the solution coming from the 3/8" tube with a certain flow rate was measured 20 cm after entering the 1/16" tube (P_1), and then, 110 cm after the turbulent flow, the pressure (P_2) was measured.

Table 2.5.3: PEG dynamic viscosity, Re and Le values at different concentrations and flow rates by the new diameter of the tube.

Conc. (ppm)	Flow Speed (L/min)	Dynamic Viscosity (mm²/s)	3/8" Tube Re Value Re=4Q/πDv	1/16" Tube Re Value Re=4Q/πDv	3/8" Tube L_e Value Le/D=$4.4Re^{1/6}$	1/16" Tube L_e Value Le/D= $4.4Re^{1/6}$
100	1	1.09	2035.32	12211.97	~~	~~
	1.5		3052.99	18317.95	15.96	3.58
	2		4070.65	24423.94	16.74	3.76
	2.5		5088.32	30529.92	17.38	3.90
	3		6105.98	36635.91	17.91	4.02
	3.5		7123.65	42741.90	18.38	4.13
	4		8141.31	48847.88	18.79	4.22
50	1	0.99	2232.91	13397.49	~~	3.40
	1.5		3349.37	20096.23	16.21	3.64
	2		4465.83	26794.97	17.00	3.82
	2.5		5582.28	33493.72	17.65	3.96
	3		6698.74	40192.46	18.19	4.08
	3.5		7815.20	46891.22	18.66	4.19
	4		8931.66	53589.96	19.09	4.28

Conc. (ppm)	Flow Speed (L/min)	Dynamic Viscosity (mm²/s)	3/8" Tube Re Value Re=4Q/πDv	1/16" Tube Re Value Re=4Q/πDv	3/8" Tube L_e Value Le/D=$4.4Re^{1/6}$	1/16" Tube L_e Value Le/D=$4.4Re^{1/6}$
10	1	0.93	2394.15	14364.94	~~	~~
	1.5		3591.23	21547.41	16.40	3.68
	2		4788.31	28729.88	17.20	3.86
	2.5		5985.39	35912.35	17.85	4.01
	3		7182.47	43094.82	18.40	4.13
	3.5		8379.55	50277.30	18.88	4.24
	4		9576.63	57459.77	19.31	4.33
1	1	0.97	2286.88	13721.2	~~	3.41
	1.5		3430.31	20581.91	16.27	3.65
	2		4573.75	27442.55	17.07	3.83
	2.5		5717.19	34303.19	17.72	3.98
	3		6860.63	41163.83	18.26	4.10
	3.5		8004.08	48024.47	18.74	4.21
	4		9147.52	54885.11	19.16	4.30

Table 2.5.4: AVDRP dynamic viscosity, Re and Le values at different concentrations and flow rates by the new diameter of the tube.

Conc. (ppm)	Flow Speed (L/min)	Dynamic Viscosity (mm²/s)	3/8" Tube Re Value Re=4Q/πDv	1/16" Tube Re Value Re=4Q/πDv	3/8" Tube L_e Value Le/D=$4.4Re^{1/6}$	1/16" Tube L_e Value Le/D=$4.4Re^{1/6}$
100	1	0.99	2241.31	13447.91	~~	~~
	1.5		3361.97	20171.86	16.22	3.64
	2		4482.63	26895.82	17.01	3.82
	2.5		5603.29	33619.77	17.66	3.96
	3		6723.95	40343.73	18.20	4.09
	3.5		7844.61	47067.70	18.68	4.19
	4		8965.27	53791.66	19.10	4.29
50	1	0.94	2348.11	14088.68	~~	3.43
	1.5		3522.17	21133.02	16.34	3.67
	2		4696.22	28177.37	17.15	3.85
	2.5		5870.28	35221.71	17.80	3.99
	3		7044.34	42266.05	18.34	4.12
	3.5		8218.40	49310.40	18.82	4.22
	4		9392.45	56354.75	19.25	4.32
10	1	0.98	2263.64	13581.89	~~	3.41
	1.5		3395.47	20372.83	16.24	3.65
	2		4527.29	27163.78	17.04	3.82
	2.5		5659.12	33954.73	17.69	3.97
	3		6790.94	40745.67	18.23	4.09
	3.5		7922.77	47536.63	18.71	4.20
	4		9054.59	54327.58	19.13	4.29
1	1	0.91	2445.00	14670.04	~~	3.45
	1.5		3667.51	22005.06	16.45	3.69
	2		4890.01	29340.09	17.26	3.87
	2.5		6112.51	36675.10	17.92	4.02
	3		7335.02	44010.13	18.47	4.15
	3.5		8557.52	51345.16	18.95	4.25
	4		9780.03	58680.18	19.38	4.35

In the modified system, the largest Reynolds number we could reach 58680 at 4L/min. The Reynolds number calculated by reducing the tube radius indicates that larger turbulence was generated.

2.6 Hemolysis

To study the hemolysis of the AVDRP and AVDRP/F, 4 mL of a blood sample was collected from a volunteer into EDTA coated tubes. Blood samples were centrifuged (Thermo scientific, SL 16R) at 3500 rpm for 5 minutes. The point where plasma separates from RBC and also, the maximum height of the plasma was marked. The plasma was removed, and 0.15M saline solution was added until the upper mark. RBCs and saline solution were gently mixed followed by centrifuge again using the same protocol. This procedure was performed to agitate the RBCs. It was repeated three times. After the third agitation, the saline solution was removed using the centrifuge, and this time 100 mM phosphate buffer saline (PBS) was added until the same mark. This solution was accepted as a stock solution for the experiment. The stock solution was diluted by 10%, and the new solution was called the working solution. More specifically, 1 mL of the stock solution and 9 mL PBS were gently mixed in a 15 mL falcon tube. It was a working solution. In a 2 mL eppendorf tube, 200μL of the working solution was mixed with solutions of AVDRP, AVDRP/F, PEG, each with concentrations of 0.1 mg/mL 0.05 mg/mL, and, 0.01 mg/mL and 0.001 mg/mL, all prepared in 1X PBS. The final volume was 1 ml in all tubes. While negative control was with only RBCs in PBS, positive control was containing a solution of 5% Triton X in PBS. All tubes were gently shaken so that the RBCs mix with the polymer solutions. Afterwards, each solution was prepared as a triplicate. The solutions were placed in a water bath at 37°C for one hour. The solutions were then again centrifuged at 5000 rpm for 5 minutes. The intact and ruptured RBCs were accumulated at the bottom in the form of a pellet. On the other hand, supernatant contained the released hemoglobin from the ruptured RBCs. 200 μL of supernatant was transferred into a 96 well-plate. Then, the absorbance of the supernatants was measured at 541 nm using a 96 well plate reader (SpectraMax® i3).

The percentage hemolysis was calculated according to the following equation:

$$\% \ Hemolysis = \frac{Absorbance \ of \ sample - Absorbance \ of \ negative \ control}{Absorbance \ of \ positive \ control} * 100 \quad (Eq \ 2.6.1)$$

where negative control contains only the RBCs with PBS, while positive control contains RBS with PBS and Triton X-100.

2.7 In vivo Studies

Male and female New Zealand rabbits (n=8, 2 to 3kg) were obtained from Istanbul Medipol University Medical Research Center (MEDITAM, Turkey). All animals were acclimated for 2 weeks before the experiment. All animals were treated in accordance with animal welfare. Rabbits were randomly selected with eight rabbits in each group. To anesthetize rabbits, ketamine hydrochloride (80 mg/kg) /xylazine (20 mg/kg) was performed via IM injection and then anticoagulated with sodium heparin (SQ, 10 IU). Rabbits were kept on the heating pad throughout the experiment. The animals were allowed to breathe spontaneously under anesthesia. Since the eyes of rabbits are large and thus, they have the risk of damage or dryness of the cornea during the operation. Before the surgery, the rabbit's eyes were protected by applying eye ointment (Terramycin[®]). Subsequently, both right and left femoral arteries were cannulated by using a 24G cannula (Neocan[TM]). While mean arterial blood pressure (MAP) was monitored from the right femoral artery by using VITA v12 Modular Monitor, the left femoral artery was used for bleeding. The right marginal ear vein cannulated with a 22G cannula for resuscitation. Laser speckle imaging (LSI, Perimed) was placed onto the left ear to continuously monitor tissue perfusion. Furthermore, pulse oxymetry (Masimo neonatal sPO_2 adhesive sensor) was placed on the arm of the rabbit for monitoring sPO_2. The resuscitation fluids was given back as two times the amount of blood drawn and PEG, AVDRP and AVDRP/F concentration was arranged as 10 ppm final concentration in whole body. The total blood volume of rabbit was calculated using the information of 54ml/kg according to literature [37]. Resuscitation was carried out throughout 15 min and this point was accepted as R_{15}. In addition, at each time point; T_b (basal value), T_i (beginning of the operation), T_0 (beginning of shock), T_5 (5 min. shock), R_0 (before resuscitation), R_{15} (after resuscitation) and R_{2h} (end of 2 hours) both blood gas analysis by i-STAT Blood Gas Analyzer using CG4+ cartridge and viscosity analysis by Brookfield DV2T Viscometer were performed.
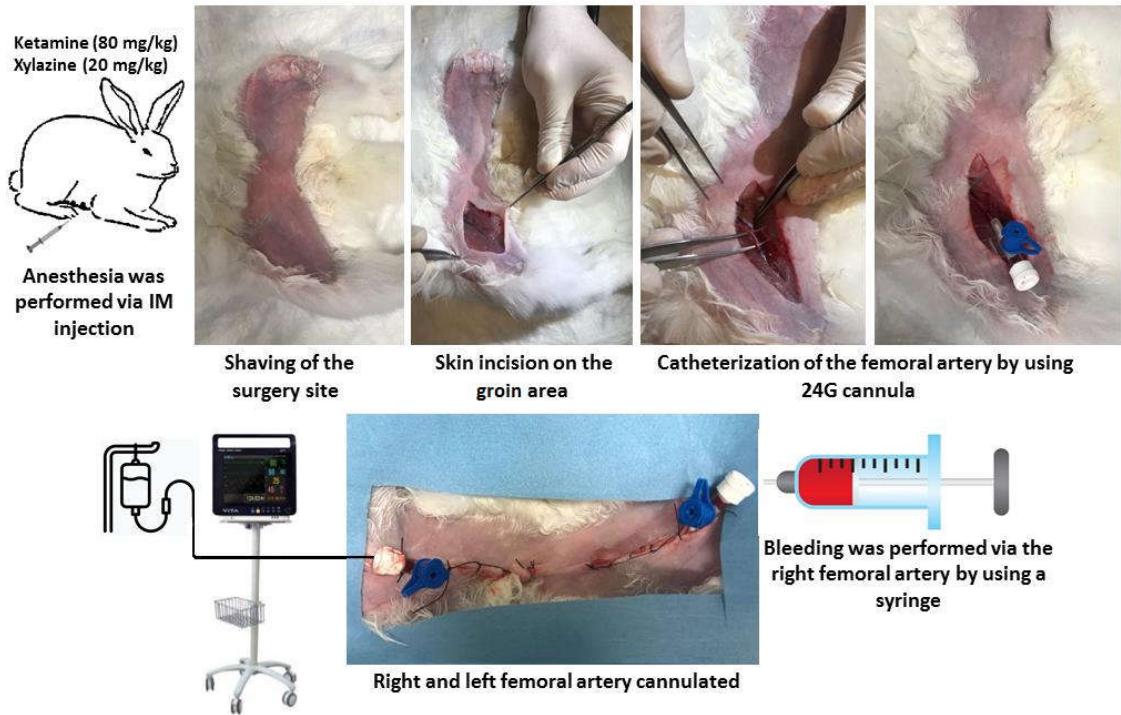
Figure 2.7.1: Surgery procedures of the rabbit
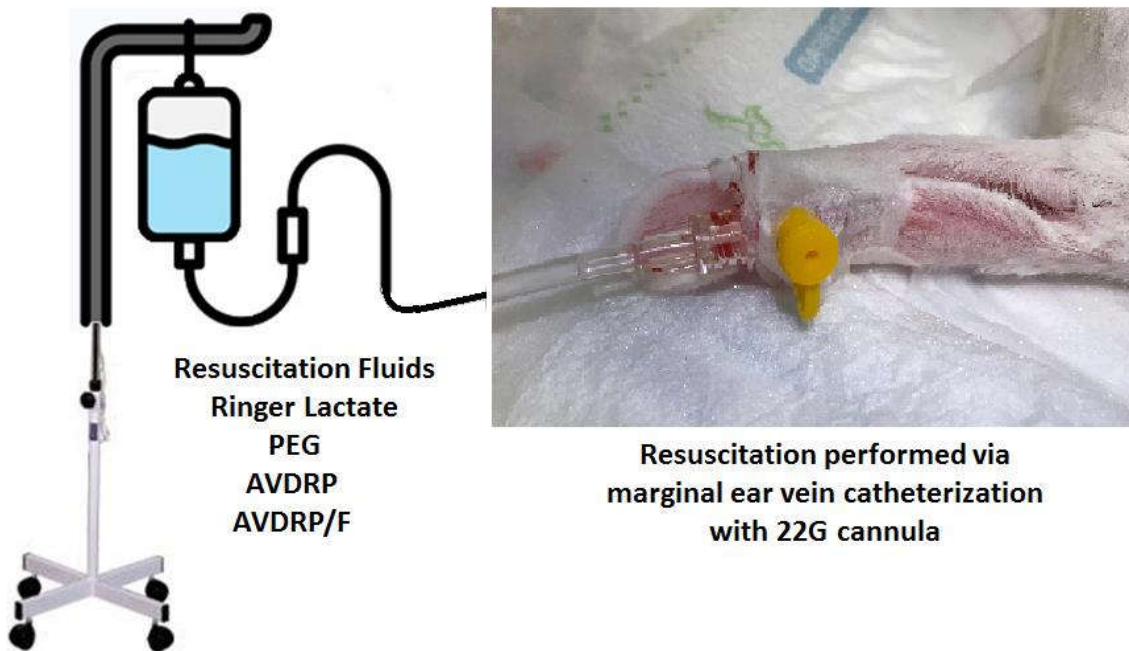
Figure 2.7.2: Resuscitation was performed via marginal ear vein

Figure 2.7.3: Laser Speckle Imaging system was placed onto ear of the rabbit

Figure 2.7.4: General view of the operation room.

2.8 Statistics

Data were presented as means ± SEM by using two-way ANNOVA followed by the Tukey test for multiple comparisons between four groups of mean arterial pressure and blood gas analysis. The three-way ANOVA was used to analyze comparisons of

viscosities of different time points for all groups. $P < 0.001$ and $P < 0.05$ were considered statistically significant. Statistical analyses were performed with GraphPad Prism 8.0.2.

Chapter 3

Results and Discussion

3.1 Extraction of Drag Reducing Polymer

The project aimed to develop of a blood supply product to use instead of classical resuscitation agent during hemorrhagic shock. Drag reducing polymers (DRP) are blood soluble long chains with high molecular weight have significant effect on blood circulation even if it is added very small concentration into blood. This high molecular weight polymer was extracted from aloe-vera plant that they were cultivated in Turkey. To obtain DRP, aloe-vera leaves were peeled off and gel was collected. Afterwards, to make homogenization, gel was mixed via overhead stirrer at 50°C for 2h followed by overnight stirring at room temperature. After gel was centrifuged, supernatants were collected and vacuum distillation was made to remove excess water content at low temperature (45°C), 100 mbar. Subsequently, dialysis were came through to make more purified sample as it helps to remove small molecular weight impurities from the system. As a final dialyzed sample was freeze dried. At every stage, DRP molecular weight was measured by using gel permeation chromatography equipped with light scattering detectors. For GPC analysis, 0.5 M ammonium acetate buffer (pH = 5.5) was used as the mobile phase. DRPs also were prepared at a concentration of 3 mg / ml in 0.5 M ammonium acetate buffer (pH = 5.5) and stirred overnight at 700 rpm. GPC analysis is performed after filtering by a 0.45 μm syringe filter. The molecular weights of AVDRP detected by GPC were between 2×10^6 - 3.6×10^6 Da using the help of dn/dc value of 0.11. Even though extraction of aloe-vera polymer was repeated more than 10 times, molecular weight was never resulted as higher than 3.6×10^6 Da. This could be possible highest molecular weight that can be reached from the plant grew in Turkey. It is known that molecular weight of the plant extract affected by climate and other properties of the region. Given the fact that DRP with the molecular weight of 1×10^6

Da or higher can exhibit drag reducing effect, obtained molecular weights are more than enough to show drag reducing effect.

3.2 Synthesis of Fluorinated DRP

Another aim of this study to enhance oxygen delivering capacity of AVDRP which already has its own mechanism to increase tissue perfusion. It was hypothesized that if a chemical structure that enhances the solubility of oxygen in blood is incorporated into AVDRP, it might increase the chance of transferring more oxygen into tissue due to its own mechanism of increasing oxygen delivery by reducing the plasma region.

There are two types of oxygen transport systems with known or even commercialized versions; hemoglobin based oxygen transport systems and perfluorocarbons. Hemoglobin-based systems have difficulties in isolation, purification, and use, but perfluorocarbon-based oxygen transport systems are more readily available and capable of releasing oxygen in a physiological environment. That's why a perfluorocarbon based oxygen transport system was chosen. Commercially available fluoroalkyl chains containing different numbers of F atoms of different lengths were integrated in a large molecular weight polysaccharide chain, aloe-vera-based DRP, via esterification over primary alcohol groups. In practice, hydrophobic perfluorocarbons are generally used as emulsions because they do not mix with water. For our system, even though when number of F increases, more available oxygen is expected to be present in the solution, it need special care to keep the balance between hydrophobic/hydrophilic structure. A systematic study was performing using different fluoroalkyl chain length and conjugation % (Table 3.2.1).

Table 3.2.1: Represents conjugation % depending on fluoroalkyl chain length

Perfluorocarbon (PFC)	F atom number	Conjugation %	State
Pentafluoro-propionic acid	**5**	20[*]	-
		10[*]	-
		5	√
		2.5	√
		1	√
Heptafluoro-butyric acid	**7**	10[*]	-
		2.5	√
		1	√
Perfluoro-pentanoic acid	**9**	10[*]	-
		2.5	√
		1	√
Undecafluoro-hexanoic acid	**11**	20[*]	-
		10[*]	-
		2.5	√
		1	√

* Esterified using DCC/DMAP system. ("-" displays precipitated/nonsoluble and "√" shows soluble)

The resulting polymers were characterized in a similar manner to AVDRP polymers. Although these functional polymers have not the same molecular weights with AVDRP's, they give a different distribution according to the starting area of the refractive index detector signal as shown in Figure 3.2.1, indication the chemical functionalization. All fluorinated DRP's molecular weights were over 1.7×10^6 Da after functionalization. As can be seen in Table 3.2.1, maximum w/w functionalization that gives the soluble product is %5. Longest F containing chain could be expected to provide more oxygen in solution, however longer chains may disturb the linearity of the AVDRP chains which is the essential components of DRP. On the other site, shorter chain will not have this problem, but they may end up having low oxygen carrying capacity. For this reason, fluoroalkyl chain containing 9 F atoms was chosen as AVDRP/F to carry animal experiment that has minimum risk of mentioned problems.
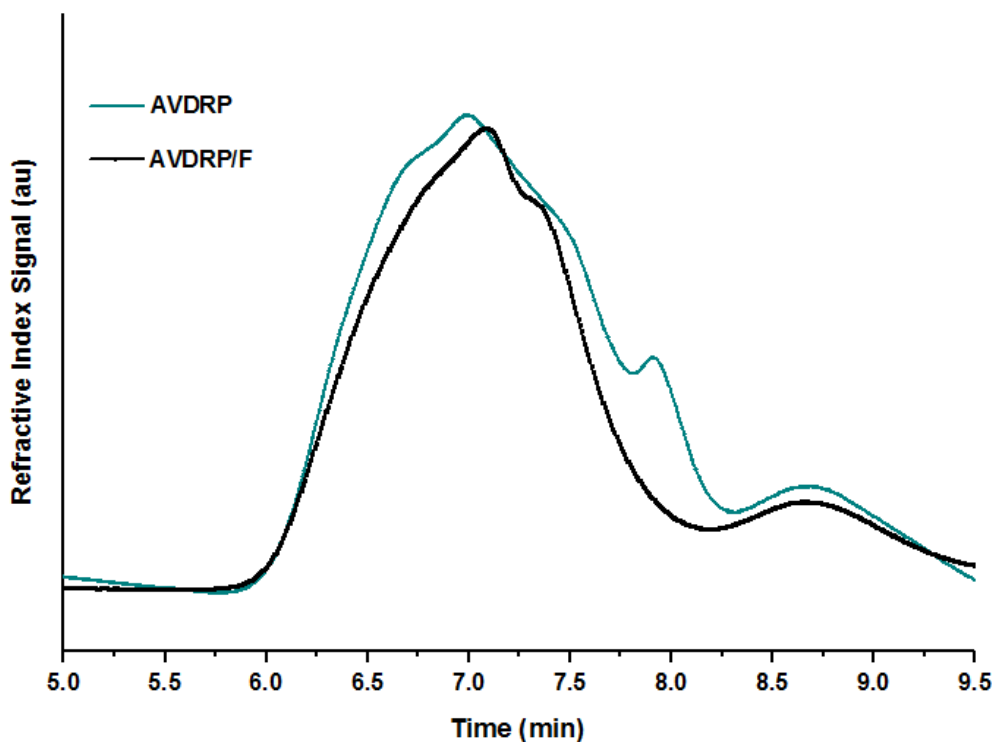
Figure 3.2.1: Comparison of refractive index graphics with AVDRP and AVDRP/F.

The ^{1}H-NMR spectra of the fluorinated polymers were compared with AVDRP. The chemical structure of the AVDRP polymer is not clearly known [36]. They are generally derived from mannose in the literature and shown in Figure 2.4.1 [38] [36] [35]. So, in this study, it was planned to perform the esterification reaction of hydroxyl groups of mannose derivatives (Figure 2.4.1). After the esterification reaction, shifts are expected in the methyl protons close to the ester group, however it is really difficult to see peek shift for such a big polymer chains in ^{1}H-NMR. The only peak difference at 8.31 ppm is observed in the ^{1}H-NMR spectrum as weak signal which could be indication possible amidation reaction (Figure 3.2.2). Generally, NH protons are observed at this ppm after amidation. This has been interpreted to mean that AVDRP may also contain mannosamine in structure and amidation under esterification conditions may also occur through amine (NH_2).
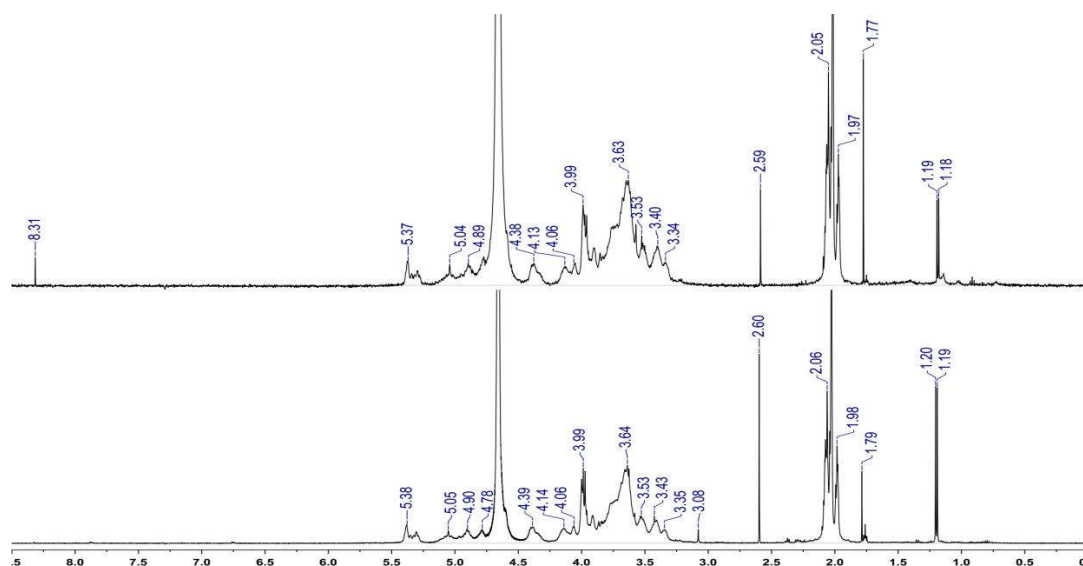
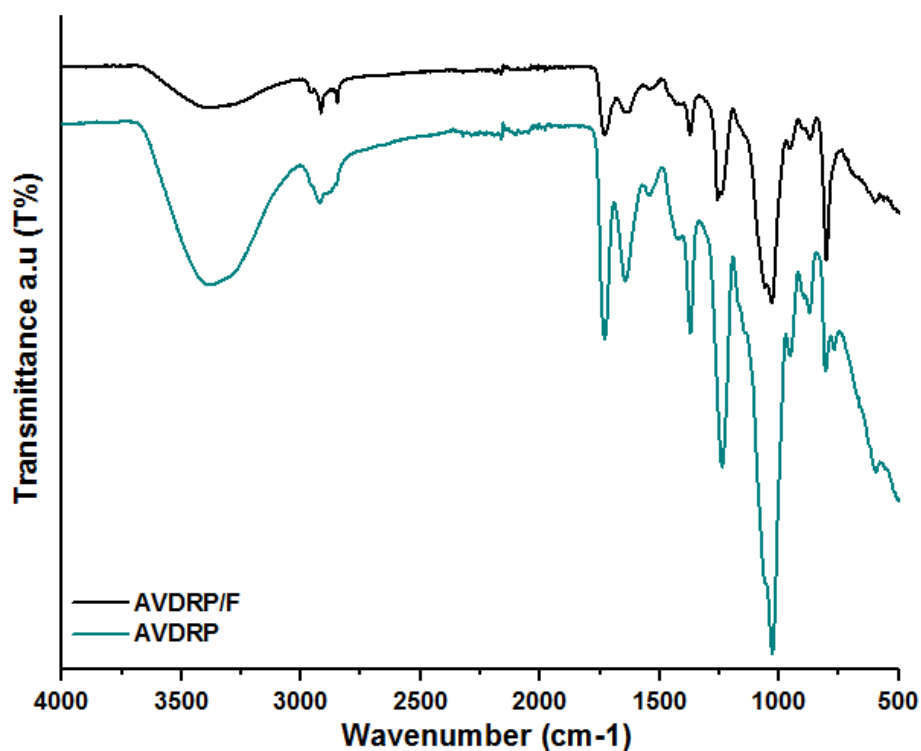**Figure 3.2.2:** ^{1}H-NMR spectrum of AVDRP/F (top) and AVDRP (bottom).

^{19}F-NMR analysis which is more characteristic for fluorinated compounds was performed; CF$_2$ and CF$_3$ fluorines of pentafluoro-propionic acid having five fluorine groups were determined to provide areas proportional to their F number. This was considered to be evidence that F-containing alkyl chains were conjugated to the main chain (Figure 3.2.3).
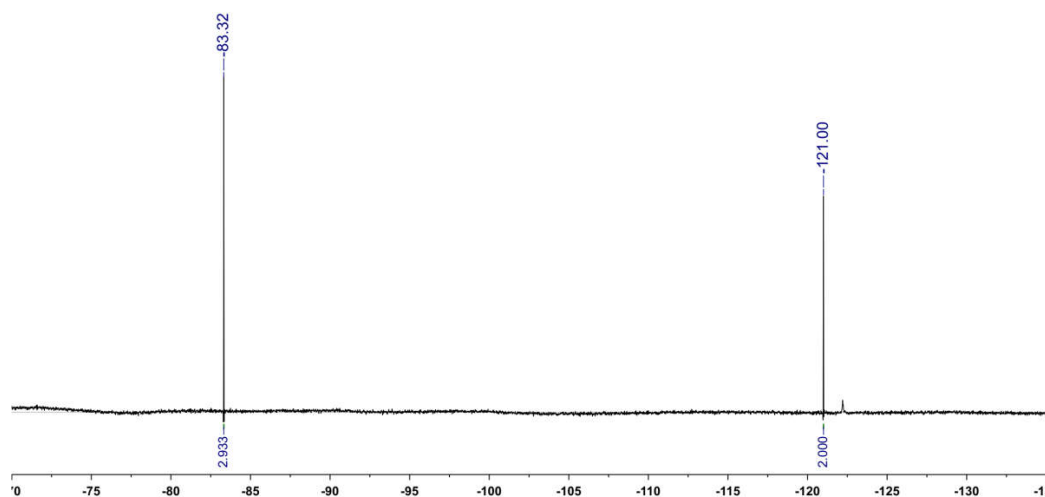
Figure 3.2.3: ^{19}F-NMR spectrum of the AVDRP/F5

Fourier Transform Infrared Spectrophotometer (FTIR) analysis of AVDRP and AVDRP/F samples are shown in the Figure 3.2.4. The decrease in the peak intensity of OH group indicates that they have been used during fluorination. Similar with AVDRP and AVDRP/F contains carbonyl signals at 1740 and 1630 indicating the presence of ester and amide groups in the structure, respectively (Figure 3.2.4). C-F bonds are

generally observed around 1200 cm-1 and this region is not very selective and coincides and cannot be detected clearly.

Figure 3.2.4: FTIR spectrum of AVDRP and AVDRP/F

The thermal properties of the AVDRP/F modified with fluorocarbon chains were compared with the initial AVDRP using the thermal weight analysis method. This is a supportive analysis that functionalization takes place through the effect of structural differences on thermal behavior after fluorination. As can be seen in Figure 3.2.5, AVDRP/F, AVDRP exhibited a different thermal behavior.
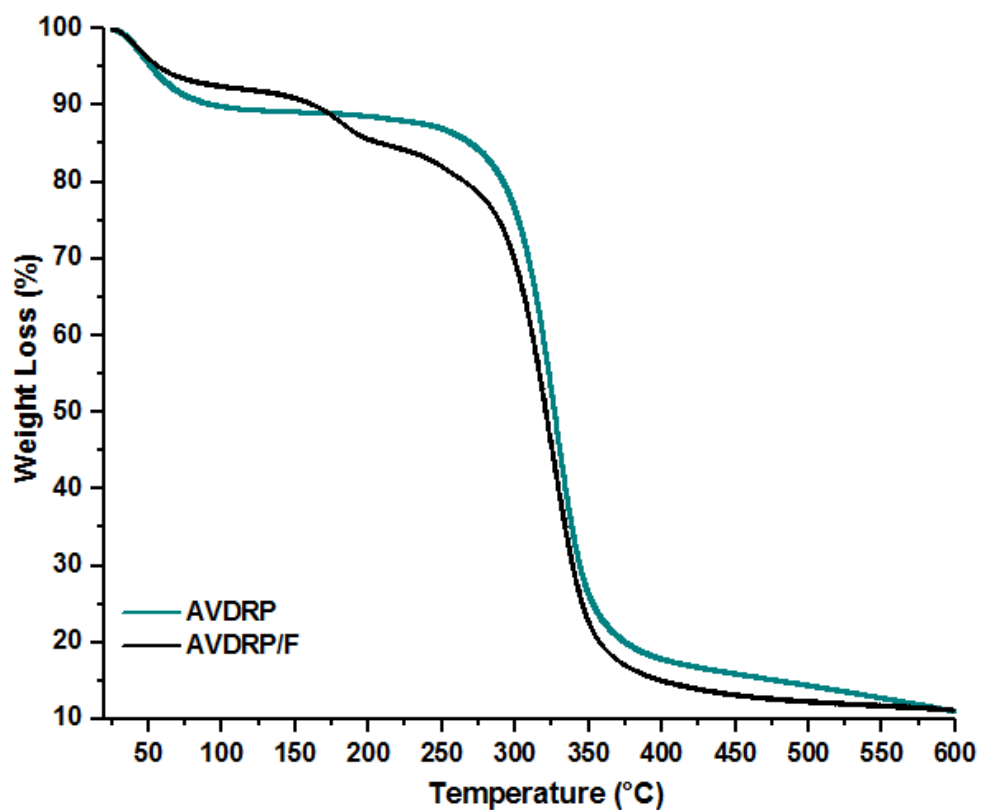
Figure 3.2.5: TGA graphics of AVDRP and AVDRP/F

Characterization of AVDRP/F was continued with elementary analysis by scanning electron microscopy and EDAX (energy-dispersive X-ray spectroscopy) detector. As shown in Figure 3.2.6, AVDRPs show more leafy morphology, while AVDRP/F has become more fiber-like after fluorination.
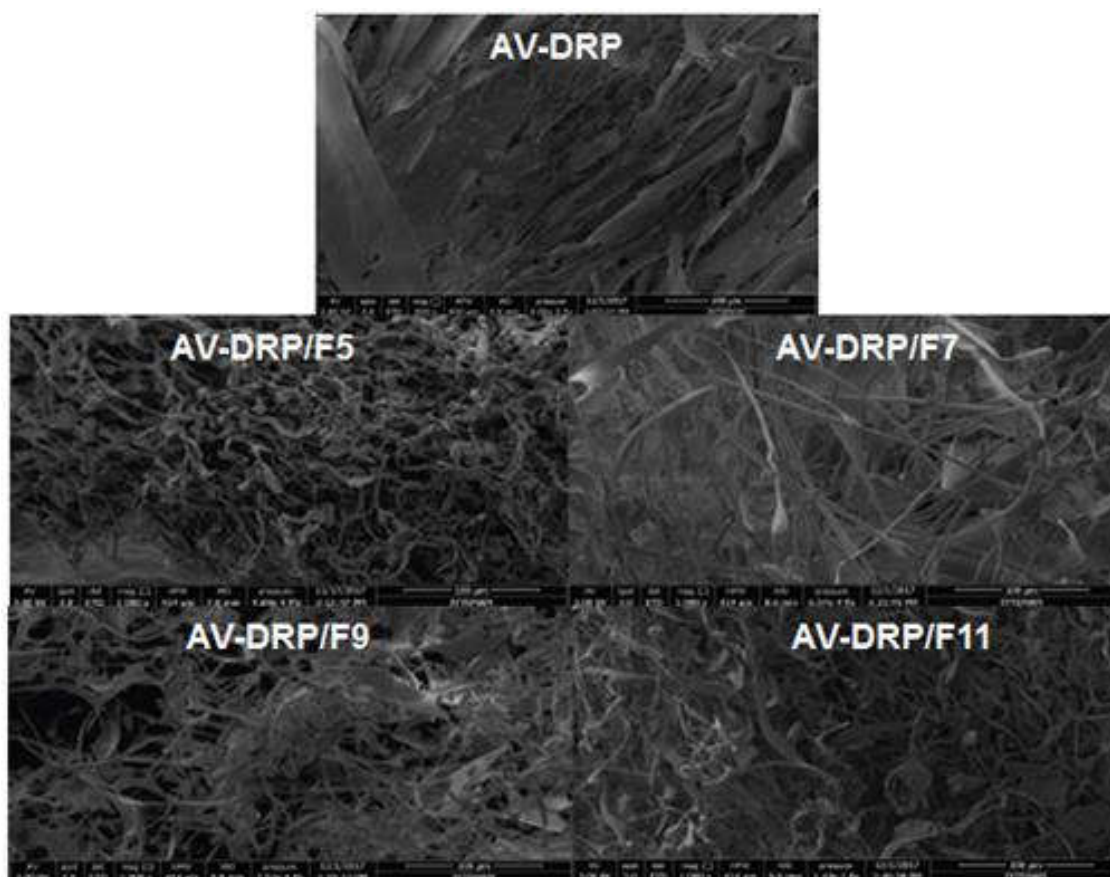
Figure 3.2.6: SEM images of AVDRP and AVDRP/F

EDAX analysis is a kind of elemental analysis and the percentage of the mass of elements in the polymer can be determined. According to the results obtained the weight percentage of F atoms increases in the polymer, when the number of F atoms increases in the fluoroalkyl chain which is conjugated into AVDRP (Table 3.2.1).

Table 3.2.2: EDAX data showing % fluorine content in AVDRP/F

Element	wt % AVDRP	wt % AVDRP/F5	wt % AVDRP/F7	wt % AVDRP/F9	wt % AVDRP/F11
C	50.57	53.58	51.04	49.77	50.6
O	49.43	42.79	47.1	48.66	47.63
F	0	0.57	1.18	1.58	1.77

3.3 Biocompatibility of AVDRPs

Since AVDRP and AVDRP/F were administered intravenously to the body, hemolysis assay was used to determine the biocompatibility of materials. Hemolysis means the breaking down red blood cells and hemoglobin is released into the bloodstream. For this reason, whether the materials have a hemolytic effect on red blood cells was measured quantitatively by hemoglobin absorption. All AVDRP and AVDRP/F polymer showed hemolytic activity smaller than 10 % comparing to positive control (Triton-X solution), while PEG exhibited 14 % hemolysis on RBCs (Figure 3.3.1). The results showed that increasing the hydrophobic fluorine content in the AVDRP, increases the hemolytic activity from 3% to 10%. Even the longest AVDRP/F has hemolytic activity less than PEG. The incorporated of fluoroalkyl chains in the AVDRP structure regardless of the number of F atoms is an additional proof that it does not present a disadvantage in terms of biocompatibility. Microscope image of hemolysis assay solutions showed that triton-X treated cells were hemolyzed and died, while AVDRP and AVDRP/F (Figure 3.3.2) derivatives were still viable.
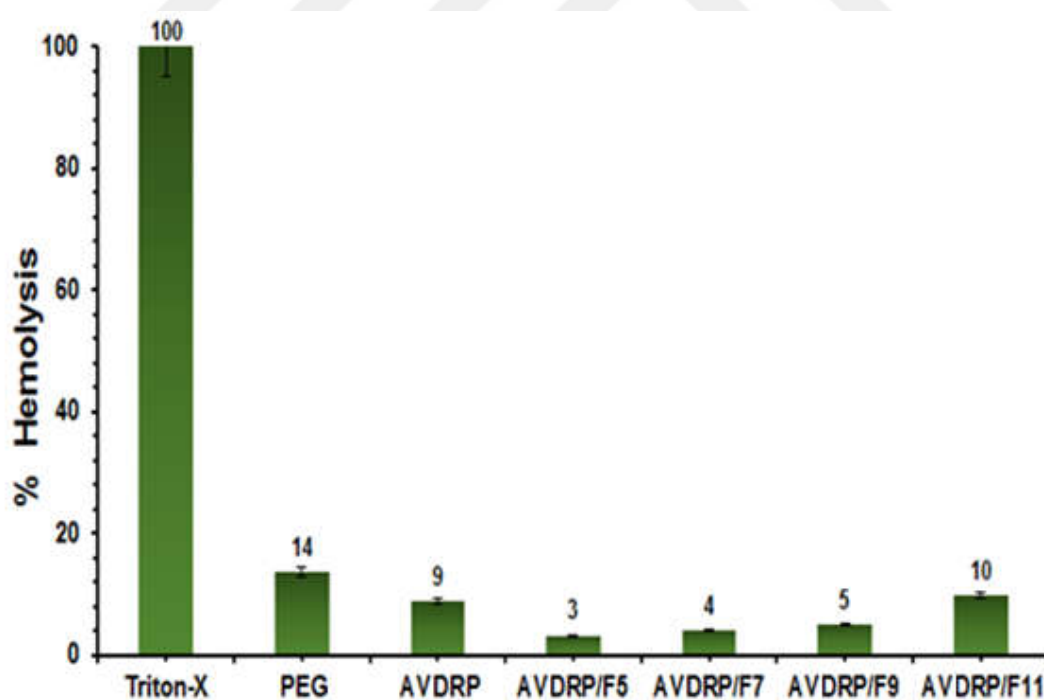
Figure 3.3.1: Hemolytic effects of PEG, AVDRP and AVDRP/F polymers by incubating with red blood cells in physiological conditions.
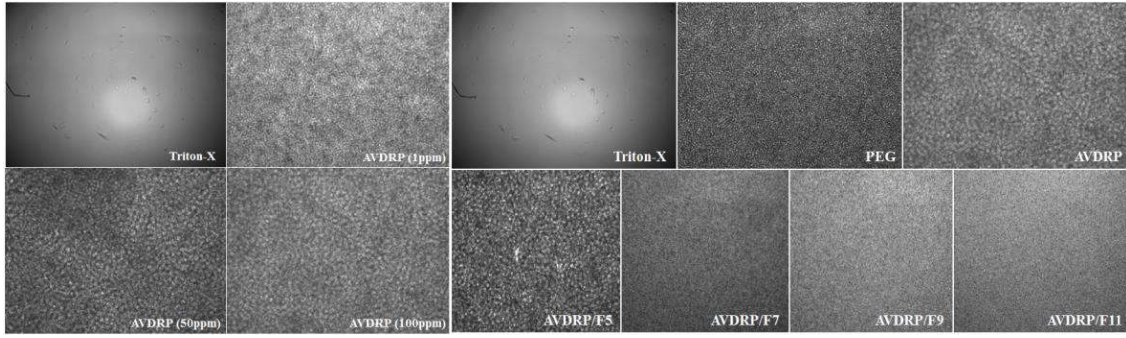
Figure 3.3.2: Microscope images of hemolysis assay solutions. While AVDRP and AVDRP/F did not produce a hemolytic effect as a result of interaction with red blood cells, those treated with Triton-X died.

3.4 Measurements of Drag Reducing Effect (DRE)

Although there is no turbulent flow in the human body, drag-reducing polymers are known to work well in a turbulent flow. A system that allows us to create turbulence flow would be the best system to test drag reducing effect of AVDRP. Thus, turbulence was created by transferring the liquid loaded in this system from a tube with a larger tube diameter (3/8") to a tube with a smaller tube diameter (1/4") and (1/16") using ECMO system. Typically, turbulence occurs if the Reynolds number is bigger than 4000. As it was explained in very detail in experimental part (section 2.5); Reynolds number was 14852 at 4L/min for 1/4" tube in our initial system. DRE effect of 50 ppm AVDRP solution was measured as 7.19% at similar Reynolds number and 4L/min flow rate (Table 3.4.1). As commercially available DRP polymer; the DRE of PEG was calculated as 16.5% in the 14220 Reynolds number at the same flow rate (Table 3.4.2). Based on literature these values were less than expected values that made us to think whether we reach the high enough Reynolds number to detect the real effect.

The drag reducing effect (DRE) was calculated according to the following formula;

$$\% \, DRE = ((\Delta P_{DRP} \; - \; \Delta P_{saline}) \, / \, \Delta P_{saline}) * 100 \qquad \text{(Eq: 3.4.1)}$$

$$\Delta P_{DRP} = P3_{DRP} - P2_{DRP} \qquad \text{(Eq: 3.4.2)}$$

$$\Delta P_{saline} = P3_{saline} - P2_{saline} \qquad \text{(Eq: 3.4.3)}$$

Table 3.4.1: Flow rate and DRE % for the 50 ppm AVDRP

Flow Speed(L/min)	$^aP_2$ (mmHg)	$^aP_3$ (mmHg)	ΔP_{2-3} (mmHg)	^bDRE (%)	Reynolds Number($4Q/\pi Dv$)(1/4"tube)
1	32	20	12	-	3517.723
2	63	27	36	2.7	7035.446
3	115	38	77	3.75	10553.17
4	276	79	129	7.19	14070.89
5	372	102	197	4.36	17588.61

$^aP_2$ and P_3 are the starting and ending pressures of the 1/4" cylinder turbulence flow.

^{b}% DRE = $((\Delta P_{DRP} - \Delta P_{saline}) / \Delta P_{saline}) * 100$

Table 3.4.2: Flow rate and DRE % for the 50 ppm PEG

Flow Speed(L/min)	$^aP_2$ (mmHg)	$^aP_3$ (mmHg)	ΔP_{2-3} (mmHg)	^bDRE (%)	Reynolds Number($4Q/\pi Dv$)(1/4"tube)
1	30	10	20	-	3555.14
2	59	18	41	-	7110.29
3	104	29	75	6.25	10665.43
4	159	43	116	16.54	14220.58
5	232	60	172	16.5	17775.72

$^aP_2$ and P_3 are the starting and ending pressures of the 1/4" cylinder turbulence flow.

^{b}% DRE = $((\Delta P_{DRP} - \Delta P_{saline}) / \Delta P_{saline}) * 100$

To create more powerful turbulence, as shown in section 2.5, Reynolds numbers were increased using smaller tube diameter. ECMO system was modified by replacing 1/4" diameter tube to 1/16" tube to have higher Reynolds numbers (shown Figure 2.5.2). This system was tested first for PEG which is the positive control polymer. As it can be seen in Table 3.4.3, DRE was measured as 29.2% in this system at the flow rate of 1 L/min and it increased to 37.3% as expected. It also noted that DRE started to decrease at higher flow rate. 4 L/min is the highest flow rate that his modified ECMO system can reach. It has very high speed flow and shear rate which most probably initiate mechanical degradation of the polymer.

Table 3.4.3: DRE of PEG (50 ppm) by modified flow rate and Reynolds number

Flow Speed(L/min)	DRE (%)	1/4" tube Reynolds Number	1/16" tube Reynolds Number
1	29.2	3517.7	13397.5
2	36.6	7035.5	26794.9
3	37.3	10553.2	40192.5
4	35.8	14070.9	53589.9

To test the mechanical degradation profile of drag-reducing polymer, the system was kept at constant and moderate flow rate (2L/min) and the change in DRE% was monitored against different time points like 5, 10 and 15 minutes (shown Table 3.5.7). A drastic decrease in DRE% was observed within 5 min as indicating the mechanic degradation of PEG. DRPs are a promising potential therapy for lots of diseases including hemorrhagic shock. On the other hand, they tend to degradation mechanically over time in high-stress conditions. In fact, this is the main limitation of DRPs. According to Dr. Kameneva and coworkers [39] mechanical degradation of DRPs may be resulting from cutting the polymer chain with mechanical stress. Mechanical degradation may also be described as a loss of drag-reducing effect of the polymer's which is not regained after removing mechanical stress. In this study, when the degradation behavior of PEG is evaluated, it can be said that it is consistent with PEG's degradation behavior shown by Kameneva and coworkers [40].

Table 3.4.4: DRE of PEG (50 ppm) by changing time at a certain flow rate (2L/min)

Time (min)	$P_{1saline}$ (mmHg)	$P_{2saline}$ (mmHg)	$\Delta P_{2\text{-}3saline}$ (mmHg)	$^aP_1$ (mmHg)	$^aP_2$ (mmHg)	$\Delta P_{2\text{-}1saline}$ (mmHg)	^bDRE (%)
0	77	12	-65	164	53	111	37.2
5	145	33	-112	227	64	163	7.91
10	245	68	-177	230	64	166	6.21
15	364	110	-254	230	63	167	5.65

^{a}P_2 and P_3 are the starting and ending pressures of the 1/16" cylinder turbulence flow.

^{b}% DRE = $((\Delta P_{DRP} - \Delta P_{saline}) / \Delta P_{saline}) * 100$

As the next step, AVDRP polymer extracted from aloe-vera was tested in the modified ECMO system to see whether an increase DRE effect will be observed or not. Before it wasn't possible to catch a turbulence flow at a flow rate as low as 1 L/min because of low Re number. However, this case DRE was calculated as 29.1% for AVDRP at the flow rate of 1 L/min. Different than commercial DRP (PEG), AVDRP had lost the DRE ability faster with the increasing flow rate. It should be mention here that, total volume of this ECMO system lowered from 1 L to 0.5 L for this system to save AVDRP polymer, and 2.5 L/min. was the highest flow rate for this system that was creating very high shear force on polymer. Similar with control polymer, a mechanical degradation can be expected from AVDRP polymer as well, but it can be claim that there was the high force on polymer under the circulation in this smaller volume and modified ECMO system. Overall, it can

be said that at possible low flow rate, higher DRE effect was observed for AVDRP in the modified system. This behavior will be further investigated in animal experiment.

Table 3.4.5: DRE of AVDRP (50 ppm) by changing flow rate and Reynolds number

Flow Speed(L/min)	^{ab}DRE (%)	1/4" tube Reynolds Number	1/16" tube Reynolds Number
1	29.1	3729.73	14088.68
1.5	4.62	7459.46	28177.37
2	1.19	11189.18	42266.05
2.5	1.22	14918.91	56354.74

^{a}P$_2$ and P$_3$ are the starting and ending pressures of the 1/16" cylinder turbulence flow.

^{b}% DRE = ((ΔP_{DRP} - ΔP_{saline}) / ΔP_{saline}) * 100

3.5 Rheological Analysis

Rheology can be described as the science of flow behavior under stress. In other words, rheology enables determining of the viscous and elastic properties of the fluids. Fluids are commonly classified as two different categories in terms of their flow behavior; Newtonian fluids and Non-Newtonian fluids. While Newtonian fluid has a linear relation of shear stress and shear rate, and also has fixed viscosity independently of the stress; non-Newtonian fluids alter their behavior of flow or viscosity under stress [41].

Rheology is required to measure viscosity and flow behavior of the fluids. It also allows us to determine the properties of the fluid we are working on based on viscosity and flow behavior. DRPs exhibit non-Newtonian flow behavior in the literature [42].

To the best of our knowledge, rheological behavior of aloe-vera extract has not been studied in detail before and a contribution on this gap in the literature was a necessity. To address this need, amplitude sweeps test made to get information about viscous and elastic behavior of the blood that contains DRP polymers. Loss modulus (G") represents the viscous portion of the mixture and it appears due to the internal frictions (energy lost) while storage modulus (G`) represents the elastic portion of the mixture. Generally, G">G` behavior shows viscous liquid with low elastic portion that typically represented by Newtonian fluid. In case G`>G"; material shows more elastic behavior which higher G` means solid like gely structure. When G' gets equal to G" (G"=G`), a flow points is observed.
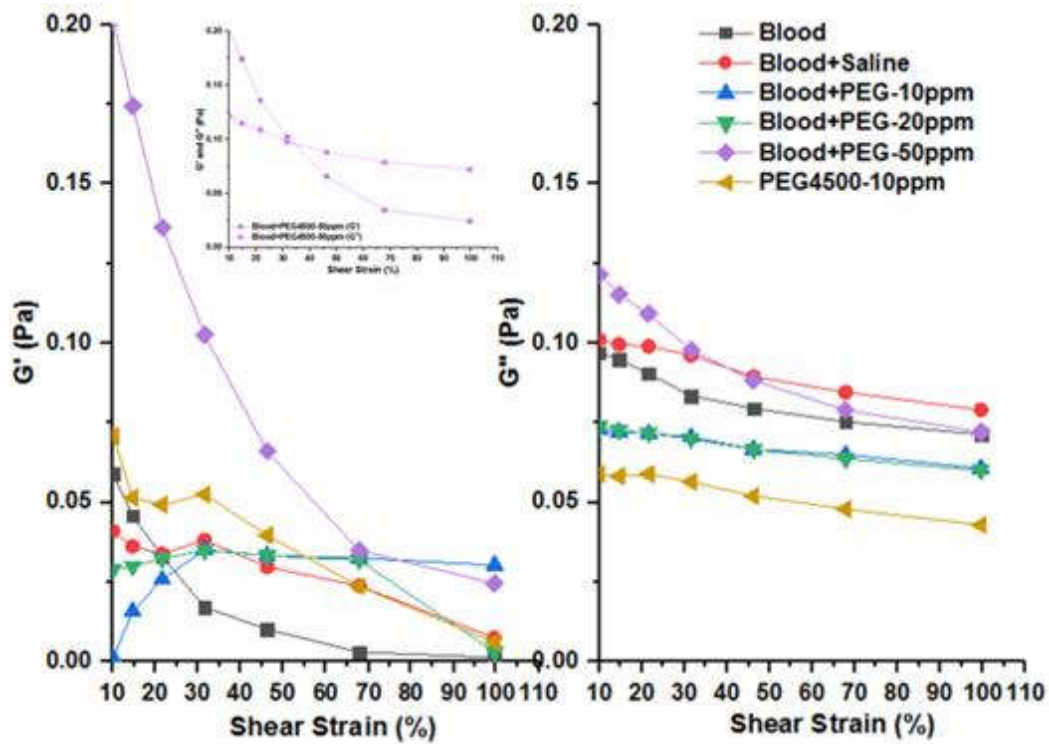
Figure 3.5.1: G' and G" (Pa) and Shear Strain (%) curves for PEG.

PEG as commercially available DRP at different concentration reflected the same behavior except highest polymer concentration. The blood mixtures at lower concentration (10 and 20 ppm) showed the viscous liquid behavior. However, once concentration increased to 50 ppm, elastic behavior got predominated at lower strain % and a flow point was observed at lower shear strain % than AVDRP sample.
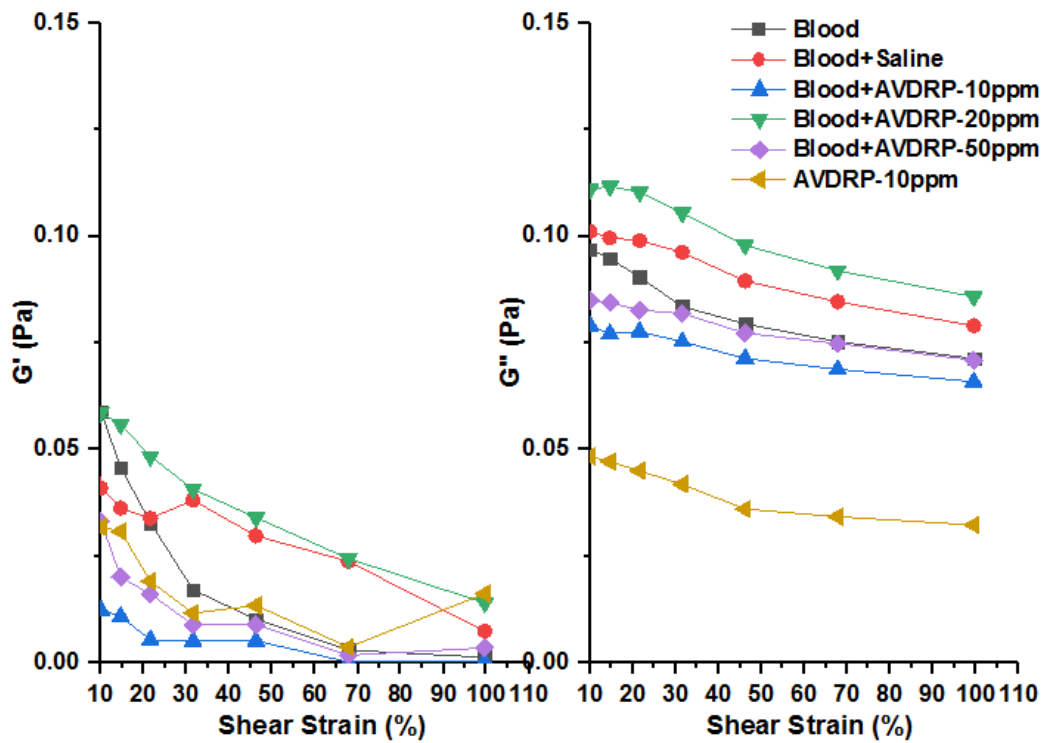
Figure 3.5.2: G' and G'' (Pa) and Shear Strain (%) curves for AVDRP.

Figure 3.5.2 shows strain dependency of the storage modulus (G`) and loss modulus(G'') for AVDRP that mixed with blood at different concentration. Similar with blood itself, all AVDRP samples exhibited higher G'' than G' which represents the viscous liquid for Newtonian fluid, although blood is mostly accepted as non-Newtonian fluid. They represent the typical drastic change for G' and slow change for G''.
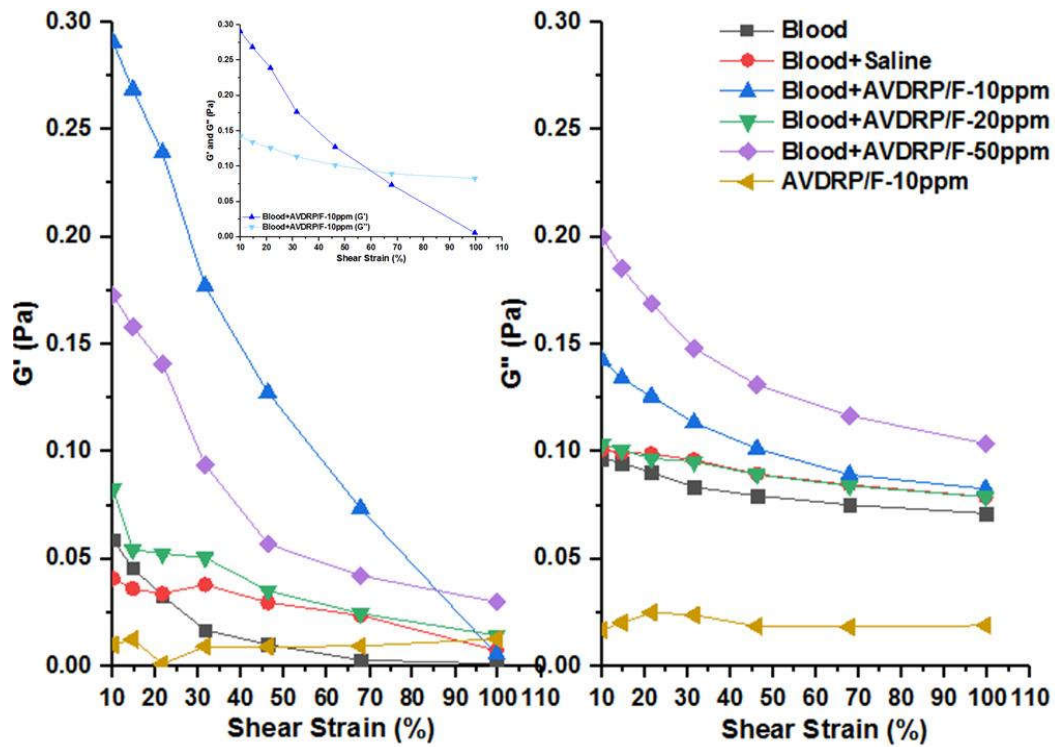
Figure 3.5.3: G' and G'' (Pa) and Shear Strain (%) curves for AVDRP/F.

Similar trend was observed for AVDRP/F samples. They mostly represent the viscous liquid behavior with higher G''. However, elastic response is predominated at lower strain for only 10 ppm solution of AVDR/F. G` value decreased by the increasing shear strain % and it crossed the G'' curve at higher shear strain %. If this was happen at higher concentration that would have a logical explanation, since expected trend was observed for 20 and 50 ppm that increasing concentration created the tendency to shift to more elastic behavior. For blood itself, blood with saline and polymer solution by itself shows opposite behavior that viscous properties are predominant than elastic properties.
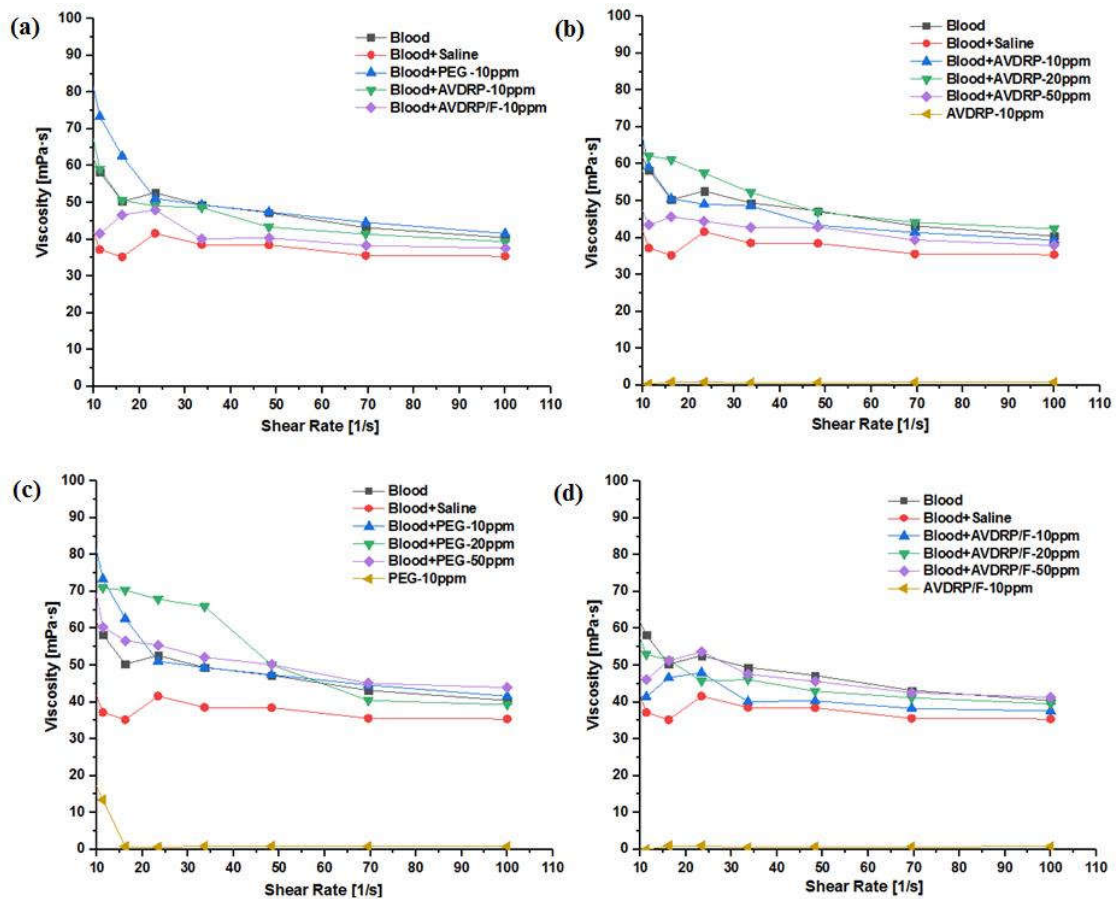
Figure 3.5.4: Viscosity (mPa.s) and Shear Rate (1/s) curves for PEG, AVDRP and AVDRP/F.

Even though recent research shows that both Newtonian and non-Newtonian model are valid for blood, and mostly accepted as non-Newtonian it is accepted that it behaves like Newtonian fluid at higher shear rate. Furthermore, it behaves like non-Newtonian at low shear rate. When all DRPs compare with the blood at different shear rate (Figure 3.5.4 (a), the viscosity of the polymer and blood have a tendency to reach a constant value. An arterial blood vessel higher than 1 mm has shear rate between 100-300 s^{-1}. Although, measurements were made between 10-100 s^{-1}, it is clear that even at higher shear rate they will keep showing Newtonian behavior. Figures 3.5.4 (b, and c, d) indicate how viscosity changes with different concentration of polymer. It can clearly be seen that increasing concentration increases the viscosity at lower shear rate, however it shows same Newtonian behavior and getting closer to same value at higher shear rate regardless of the concentration.

3.6 Hemorrhagic Shock in Rabbit

Thirty one female and male rabbits were randomly distributed in 4 groups, namely RL, PEG, AVDRP and AVDRP/F. Before starting operation, blood gas and viscosity analysis were performed for untreated animal to use it as basal value (Tb). Anesthesia was performed with ketamine hydrochloride (80 mg/kg)/xylazine (20 mg/kg) via IM injection. The additional dose was administered if it is needed. 5 min stabilization time was applied to all animal after catheterization and monitored pressure value was accepted as initial values (T_0). A fixed pressure hemorrhagic shock model was applied, and animal allow bleeding until their MAP values reached to 22 ± 2 mmHg. After shock was induced, 5 min waiting time was recorded (T_5) for all animals to see whether animal compensate the pressure loss. Additional blood was drawn to rearrange the pressure at desired value if it is needed. Even though fixed volume hemorrhagic shock model was not followed for this study; bled blood volume for all rabbits was not higher that 35% of the total blood volume of each rabbits. On the other hand, fixed pressure method allows us to compare compensation in the pressure since all of them start resuscitation at same pressure. Resuscitation was performed through marginal ear vein at the constant rate for 15 min. Resuscitation reagents were injected as 10 ppm final body concentration within the volume of twice the total amount of bled blood. % 0.9 isotonic solution was infused 10 ml/kg/h for 2 hours to recover insensible liquid loss of the animal. Changes of MAP during whole operation can be seen in Figure 3.6.1. The animals in the group of AVDRP and AVDRP/F polymers restored the higher MAP value during 15 min resuscitation. When MAP recovery compared based on the maximum MAP value that animal reached during operation, higher recovery as 97.7 % was observed AVDRP and followed by RL and AVDRP/F groups with the values of 94.4% and 91.5% with no significance, respectively. Finally, all groups had almost the same final recoveries end of the whole operation.
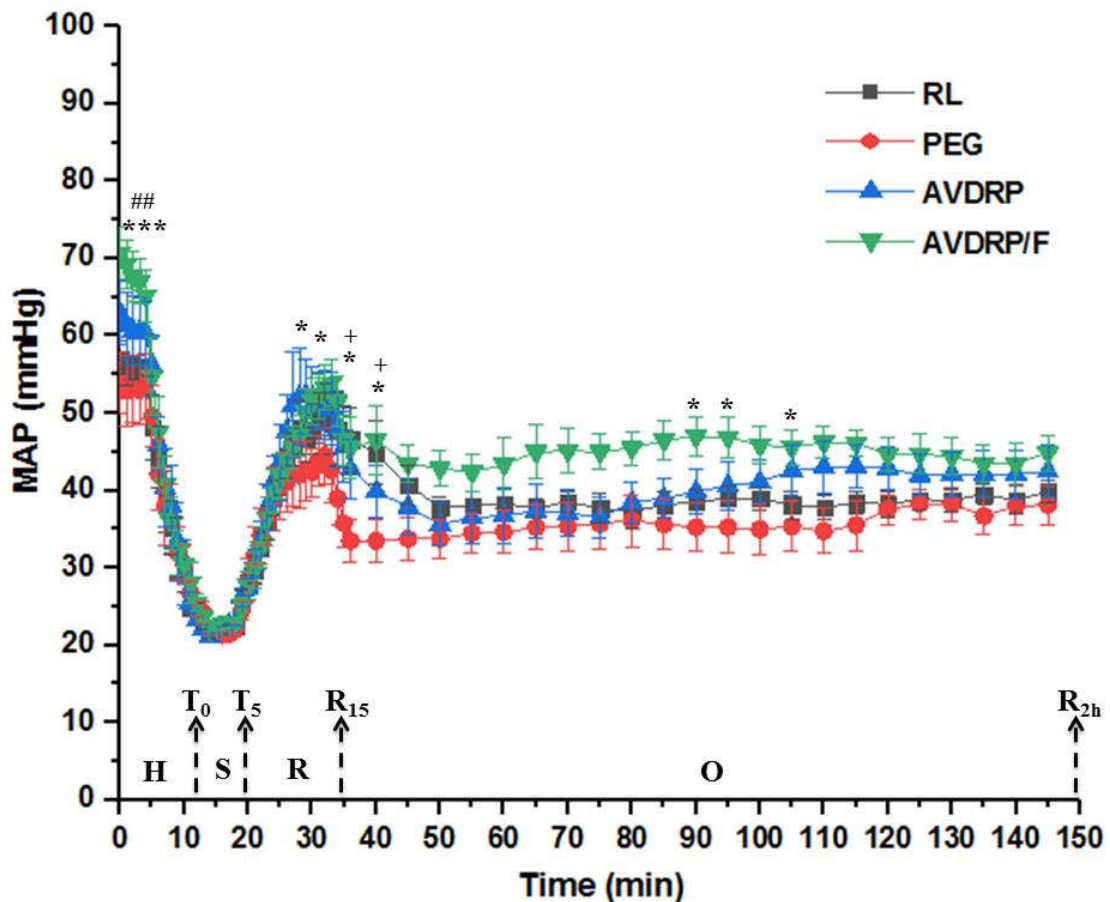
Figure 3.6.1: Impact of hemorrhage and resuscitation on mean arterial pressure (MAP) of rabbits exposed to fixed-pressure hemorrhagic shock. Data are reported as means ± SEM. (n=8). H (hemorrhage), S (shock), R (resuscitation), O (2h observation).
*$P < 0.05$ compared with PEG to AVDRP/F, ***$P < 0.001$ compared with PEG to AVDRP/F, $^{##}P < 0.005$ compared with RL to AVDRP/F, $^{+}P < 0.05$ compared with RL to PEG by using two-way ANOVA followed by the Tukey test for multiple comparisons.

Table 3.6.1: Comparison of MAP recovery

Groups	Initial MAP	Max. MAP	% Max. Recovery of MAP	Final MAP	% Final Recovery of MAP
RL	56.1	53	94.4	39.8	70.9
PEG	54	48.8	90.5	38.1	70.6
AVDRP	60.6	59.2	97.7	42.5	70.1
AVDRP/F	66.7	61.1	91.5	44.8	67.2

Initial MAP: 5 min. after catheterization. Final MAP: End of the 2h observation. Max. MAP: Animal recovers during the whole procedure after shock (T_5).

Table 3.6.2 shows detail pressure values, heart rate, body temperature and sPO$_2$ of each group based on important time points. Pressure values in this table also support the graph presented above. In addition to pressure regulation, AVDRP and especially the one has a potential to provide more oxygen in blood, AVDRP/F, may increase the oxygen amount in blood. sPO$_2$ value that helps the estimate the total oxygen amount in the blood. As can be

seen in Table 3.6.2 sPO_2 values of the AVDRP/F group end of the 2 h is higher (98.7%) than any other group and it followed by its precursor, AVDRP (98.1%). This data supports that AVDRP/F provides more soluble oxygen into blood. Since the blood that contains AVDRP derivatives in it flows closer to the vessel wall, it is expected that it will provide more oxygen into tissue. This hypothesis was also investigated via laser spackle imaging and will be discussed in the following section.

Table 3.6.2: Changes in systolic, diastolic and mean arterial pressure (MAP); and heart rate (HR), rectal temperature (RT), oxygen saturation (sPO_2)

Time	Groups	Systolic Pressure (mmHg)	Diastolic Pressure (mmHg)	MAP (mmHg)	sPO_2	HR	RT (°C)
T_i	RL	74.4±2.8	48.2±2.4	56.1±2.1	90.2±2.1	162±7	35.7±0.9
	PEG	75.8±5.3	44.25±3.6	54±4	88.5±1.6	172±3	36±0.3
	AVDRP	81.1±6.3	52±3.4	60.6±3.9	85±2.9	162±4	36.9±0.6
	AVDRP/F	85.1±4	56.2±2.8	66.7±2.6	82.2±2.8	165±5	37.3±0.5
T_0	RL	29.7±0.7	19.4±1	22.4±0.3	93.5±3	160±4	35.7±1.2
	PEG	29.8±1.6	18.3±0.8	22.1±0.3	93.3±4.5	173±4	36.9±0.4
	AVDRP	28.2±1.3	18.4±0.8	22±0.4	91.3±2.2	167±2	36.8±1
	AVDRP/F	27.8±0.5	20.7±0.5	23±0.4	89.5±2.5	175±4	37.4±0.6
T_5	RL	29.7±1.7	19.8±0.9	22.4±0.9	93±3	154±6	35.6±1.1
	PEG	30.3±0.9	18.6±1	22±0.4	93.6±3.8	163±4	36.7±0.3
	AVDRP	29.8±1	19.2±0.9	22.7±0.4	90.7±3.3	160±3	36.3±0.9
	AVDRP/F	29.7±0.9	21.3±0.5	22.8±0.4	85.6±5.5	168±5	37.3±0.6
R_{15}	RL	69.8±4	40.4±3.3	50±3.2	94±2.3	134±4	35.4±1.2
	PEG	68.3±4.3	33.2±2.6	45±3.2	97.2±0.8	150±4	36.3±0.4
	AVDRP	76±6.3	40.5±3.2	51.2±3.6	95.6±1.4	149±5	35.5±1.2
	AVDRP/F	74.2±4.6	45.5±2.8	55±2.9	94.5±2.1	154±5	37.1±0.6
R_{1h}	RL	54.8±1.6	30.5±1.3	38.5±1.4	97.1±1.4	148±11	35.8±1.3
	PEG	53.2±4.9	26.2±2.5	35.3±3.1	93.6±4	158±4	36.2±0.6
	AVDRP	55±4.8	32.2±2	39.8±2.8	97.8±0.9	168±8	36.7±1
	AVDRP/F	61.3±3	39.6±2.6	47±2.6	96.7±0.9	174±9	37.5±0.7
R_{2h}	RL	56.7±2.1	31.5±1.3	39.8±1.5	95.4±1.8	159±13	36.2±1.4
	PEG	56.7±3.6	28.7±2.1	38.1±2.4	95.7±1.3	144±10	36.4±0.8
	AVDRP	57.3±5.5	35.1±2.5	42.5±3.2	98.1±0.8	180±11	37±1.3
	AVDRP/F	57.2±4.4	37±1.6	44±2.5	98.7±0.3	189±10	37.6±0.6

Data are represented as means ± SEM. RL (n = 7). PEG (n=8). AVDRP (n = 8). AVDRP/F (n = 8). T_i (beginning of the operation), T_0 (beginning of shock), T_5 (after 5 min. shock), R_{15} (after 15 min. resuscitation), R_{1h} (end of 1 hour), R_{2h} (end of 2 hours).

Arterial blood gas results allow assessing acid-base status, gas exchange and checking of the ventilation during the operation. It also helps in indicating the delivery of oxygen to tissues. pCO_2 has the importance in terms of the acid-base balance of the respiratory component. The mean value is for the pCO_2 in rabbits is 33 mmHg. In our study, the basal value of arterial blood pH was 7.46±0.01 for all untreated animals and a slight decrease was observed for all groups while the basal values in the partial pressure of carbon dioxide (pCO_2) were 33.23±1.7 mmHg and an increase was monitored in all groups of rabbits after anesthesia. Blood gases for each group that the decrease in pH with the increase in pCO_2 is interpreted as a primary respiratory acidosis. During anesthesia, it may be related to airway obstruction or body position. In addition, airway obstruction can be observed in the cases not provided artificial airways like a tracheostomy [43]. Partial pressure of oxygen (pO_2) and partial pressure of carbon dioxide (pCO_2) showed opposite effect both at shock and end of the 2 h observation time. While pCO_2 increases with the hemorrhagic shock, pO_2 decreases for all groups. However, only AVDRP and AVDRP/F groups completed the treatment with the highest PO_2 value as 79.5 and 80.3%, respectively. Similarly, pCO_2 values are smaller and getting closer to its basal values for these groups.

The excess of base is related to the metabolic component of the acid-base balance. Base excess also has a correlation with blood pH and pCO_2. In other words, it is the amount of acid to return blood to its normal pH at a certain pCO_2 (33 mmHg for rabbits). On the other hand, there is a buffer system in the body that is able to work very fast to protect the optimum pH of the blood. The main buffer system is the cycle of carbonic acid and bicarbonate. Bicarbonate will maintain the blood pH at the normal range of 7.38 to 7.53 in rabbits. The pH<7.38, it means acidemia while the pH>7.53 alkalemia. Furthermore, BE and HCO_3^- has a good correlation in the determination of the metabolic acidosis and metabolic alkalosis. Low HCO_3^- and BE indicate metabolic acidosis and high HCO_3^- and BE show by slightly increase pH metabolic alkalosis. The normal value of HCO_3^- varies between 17.5-27.6 mmol/L in rabbits based on published data [44]. In our study; the basal values of BE and HCO_3^- were 0.33 ±1 mmol/L, 24±0.9 mmol/L respectively. During hemorrhagic shock, BE and HCO_3^- were increased with slightly decreasing pH for all groups. This demonstrates that metabolic alkalosis was revealed with hemorrhagic shock. After resuscitation, BE and HCO_3^- were getting decrease by a lower pH (pH < 7.38) especially BE in AVDRP and AVDRP/F were decreased to 2.1 ±2.2

and 2.5 ±1.6. End of the 2 h observation time, BE became more negative, HCO_3^- level decreased in AVDRP and AVDRP/F groups and get into normal range for these groups.

Because i-stat blood gas analyzer calculates the TCO_2 values depending on HCO_3^- and PCO_2 values based on Henderson-Hasselbalch equation [44] similar trend that we observed for PCO_2 and HCO_3^- are exist on total carbon dioxide level as well.

The level of oxygen saturation measured by blood gas analyzer were also supported the data obtained using pulse oxymetry showing that AVDRP and AVDRP/F groups are better on the level of oxygen saturation at the end of 2h.

Most important marker to follow hemorrhagic shock and the restoration of the body is lactate level. It is expected that lactate level increases during hemorrhagic shock and should decrease when the animal restore the shock conditions. Basal lactate level of the all animals 4.24±0.6 and it decrease with anesthesia to 2.7±0.5 to 2.1±0.4 as consistence with literature values [3]. After hemorrhagic shock was induced (T_5), lactate level increased for all animals that was accepted as an indication of the shock condition. During resuscitation (R_{15}); all DRP polymer groups including PEG restored the lactate level either by decreasing or staying at same level, while lactate level of RL group kept increasing. Even though the level of lactate did not reach the initial (T_0) value, it further decreased based on shock condition for RL and PEG groups. AVDRP and AVDRP/F groups could not continue to create same effect on lactate level that they initially performed during resuscitation. Lactate level increased at the end of the 2 h for these groups.

Table 3.6.3: Effects of resuscitation and hemorrhagic shock with PEG, RL, AVDRP and AVDRP/F on arterial blood gases

Parameter	Group	T_b	T_0	T_5	R_{15}	R_{2h}
pH	RL		7.4±0.01	7.45±0.02	7.38±0.01	7.40±0.01
	PEG	7.46±0.01	7.43±0.01	7.46±0.02	7.34±0.03	7.31±0.07
	AVDRP		7.4±0.01	7.42±0.02	7.37±0.02	7.4±0.01
	AVDRP/F		7.39±0.01	7.4±0.01	7.36±0.01	7.39±0.01
pCO$_2$ (mmHg)	RL		56.9±1.1	49.5±3	54.7±1.9	52.2±3.2
	PEG	33.23±1.7	54.3±1.5	48.5±3.4	52.2±1.9	56.9±3.7
	AVDRP		55.3±1.9	51.5±2.6	46.7±2.2	36.6±4.3[a]
	AVDRP/F		54.2±1.5	50.9±1.5	48.4±1.7	37.6±3.9[#b]

Parameter	Group	Tb (basal)	T0	T5	R15	R2h
pO2 (mmHg)	RL		56.2±2.5	73.7±6.3	65.4±4.3	69.1±1.9
	PEG	88.8±6.1	53.5±2.4	66.6±10.6	70.7±4	65.7±8.6
	AVDRP		50.6±2.4	68±4.4	69.8±2.6	79.5±5.1
	AVDRP/F		51.8±3	67.5±2	67.7±4.4	80.3±3.8
BEcf (mmol/L)	RL		11.7±1.5	11±1.7	7.2±1.8	8±2.1
	PEG	0.33±1	12.1±1.5	10.7±2	3.8±3.1	4±4
	AVDRP		10.5±1.7	9.3±1.4	2.1±2.2	-2.2±2.4*
	AVDRP/F		9±1.6	7.3±1.7	2.5±1.6	-2±2.3♯
HCO3 (mmol/L)	RL		36.4±1.3	34.9±1.5	32.5±1.7	32.8±2
	PEG	24±0.9	36.4±1.3	34.6±1.9	29.4±2.5	30.1±2.8
	AVDRP		35±1.5	33.6±1.2	27.3±2	22.6±2.4+c
	AVDRP/F		33.6±1.4	32±1.5	27.7±1.5	23±2.2Δd
TCO2 (mmol/L)	RL		38.2±1.4	36.5±1.5	34.1±1.8	34.5±2
	PEG	24.8±0.9	38±1.3	35.8±2	37.1±7.4	31.6±2.7
	AVDRP		36.7±1.6	35.2±1.3	28.7±2	23.7±2.5*
	AVDRP/F		35.1±1.4	33.5±1.6	29.1±1.5	24±2.4♯
sO2 (%)	RL		87.4±1.2	93.8±1.4	90.4±1.5	93.6±0.3
	PEG	96.2±0.8	86.6±1.5	83.2±10.6	91.5±1.3	92.1±1.7
	AVDRP		83.6±2	91.8±1.5	92.5±0.9	95.1±0.6
	AVDRP/F		83.8±2.2	92.6±0.5	91.1±1.5	95.3±0.5
Lactate (mmol/L)	RL		1.5±0.1	2.5±0.2	3.8±0.3	2.7±0.3
	PEG	4.24±0.6	2.7±0.5	4.5±1	4±1	3.2±0.2
	AVDRP		2.1±0.4	3.6±0.7	3.5±0.8	3.7±1.2
	AVDRP/F		1.9±0.4	3.4±0.3	2.6±0.3	3.9±0.3

Data presented are mean ± SEM. RL (n = 7). PEG (n = 8). AVDRP (n = 8). AVDRP/F (n = 8). Tb (basal value), T_0 (beginning of shock), T_5 (after 5 min. shock), R_{15} (after 15 min. resuscitation), R_{2h} (end of 2 hours). *$P < 0.05$ RL vs AVDRP. +$P < 0.005$ RL vs AVDRP. Δ$P < 0.005$ RL vs AVDRP/F. ♯$P < 0.05$ RL vs AVDRP/F. [a]$P < 0.0001$ PEG vs AVDRP. [b]$P < 0.0001$ PEG vs AVDRP/F. [c]$P < 0.05$ PEG vs AVDRP. [d]$P < 0.05$ PEG vs AVDRP/F. (Two-way ANOVA followed by the Tukey test for multiple comparisons)

Blood viscosity that contains AVDRP polymers was discussed earlier. At this stage, viscosity was measured for important time point as a hemodynamic parameter. Viscosity has importance in terms of vascular homeostasis. Blood viscosity is primarily correlated to plasma viscosity and the red blood cells (RBCs) concentration. Blood viscosity changes under physiological conditions such as hemorrhagic shock. During hemorrhagic shock, resulting from the loss of RBCs and plasma proteins, plasma and blood viscosity decrease sharply [45]. In this study, the basal value of the viscosity was 5.6±0.1 mPa.S and it is slightly decreased by anesthesia. As expected, blood viscosity was fell down to 4.71±0.1 mPa.S after created hemorrhagic shock. After resuscitation and end of 2 h of

observation, decreasing of the blood viscosities to 3.44±0.1 mPa.S and 3.60±0.1 mPa.S respectively was related to dilution of the blood.
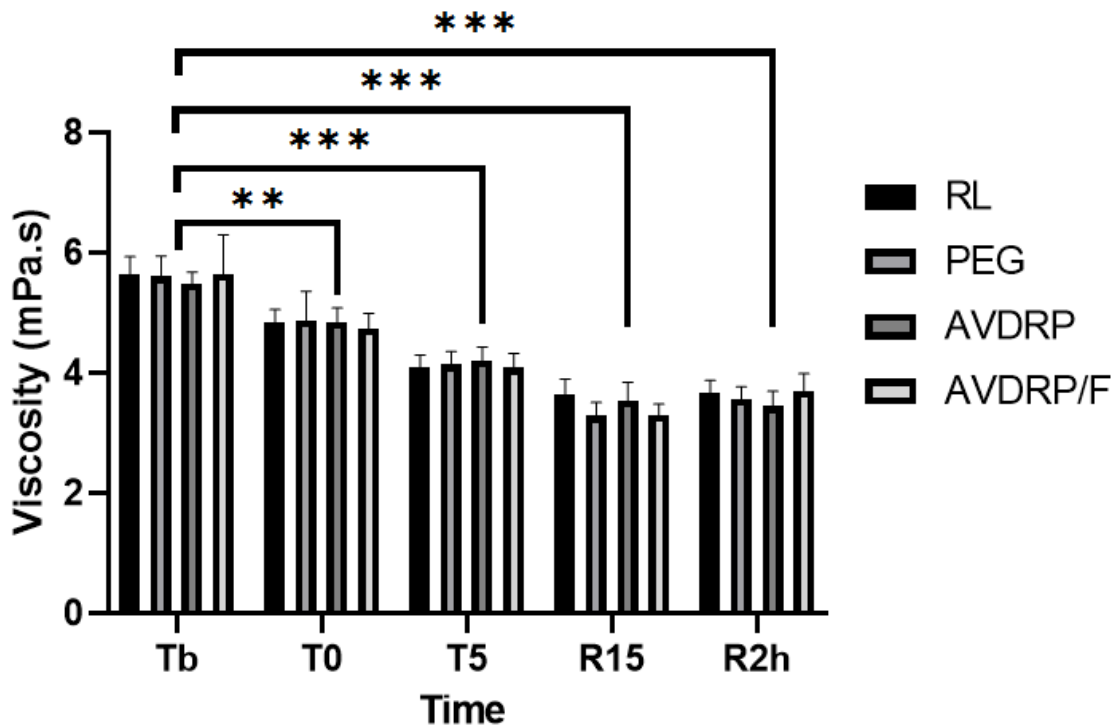
Figure 3.6.2: Viscosity measurements of each group in different time points. (Data presented are mean± SEM, n=8) *P=0.0073 and ***P<0.001 versus Tb values.
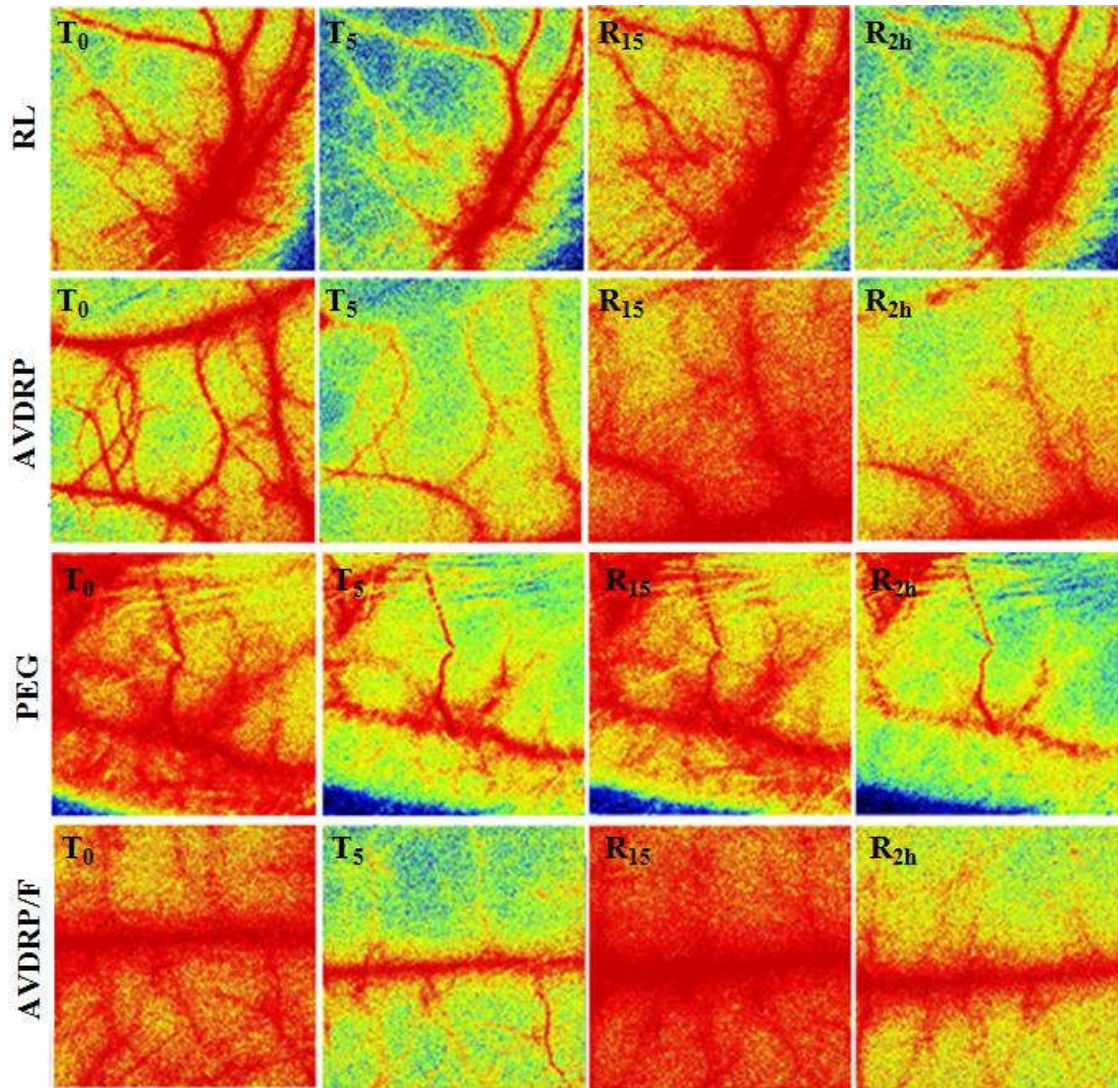
3.7 Laser Speckle Imaging (LSI)

Laser speckle imaging (LSI) system is commonly used for imaging of blood flow in animal models and clinics. Laser Speckle Imaging is a method that allows direct visualization of tissue perfusion in microcirculation. In other words, it gives information regarding the scattering particle's movement in the sample. When the laser light applied onto the region of interest (ROI) such as blood vessels, a random speckle pattern is produced by scattering of the light back from the tissue. This can be considered as creating a map of the blood flow in the tissue [47]. This random speckle pattern alters with the movement of the blood cells. When the movement of the flow is high, the altering pattern gets blurred and the contrast diminishes in that region. Therefore, low contrast is correlated with high flow and high contrast is a relationship with low flow. The contrast image is produced depending on blood flow in the tissue. While the blue color in the image represents low flow, red color indicates high flow. As a result, the intensity of the blood flow is recorded as perfusion that is calculated by the average red blood cell rate and moving red blood cell concentration [46].

In the experimental setup, working distance and the number of photos to be captured in one second were determined. Afterward, the ear of the rabbit was illuminated by laser light and images were captured by a digital camera. Processed images by software enable to screen speckle pattern in the object such as red blood cells and the speckle pattern changes with the flow of the blood in the vessel or movement of the red blood cells in the blood. Accordingly, tissue perfusion was calculated by the software via the resulting contrast difference.

In this study, tissue perfusion and oxygenation were investigated by using LSI. Figure 3.7.1 indicates captured images at different time points as T_0, T_5, R_{15}, and R_{2h}. As anticipated that the blood flow intensity was significantly lowered after hemorrhagic shock for all groups (n=8). After fluid resuscitation, there were significant changes in the intensity of the blood flow in each group. AVDRP and AVDRP/F blood flow intensity remarkably increased compared to PEG and RL. Then, this increase also was better, in the same way, the end of 2h than PEG and RL.

Figure 3.7.1: Laser speckle images of RL, PEG, AVDRP and AVDRP/F. (T_0 (beginning of shock), T_5 (after 5 min. shock), R_{15} (after 15 min. resuscitation), R_{2h} (end of 2 hours))

Tissue perfusion is expressed by blood flow in the laser speckle imaging system (shown in Figure 3.7.2). Similarly, with reduced blood flow, tissue perfusion is reduced after hemorrhagic shock. Compared to the RL group, fluid resuscitation significantly improved blood flow intensity and tissue perfusion in every group. In particular, AVDRP and AVDRP/F not only sustained this improvement in tissue perfusion but also achieved highest tissue perfusion until the end of the 2h.
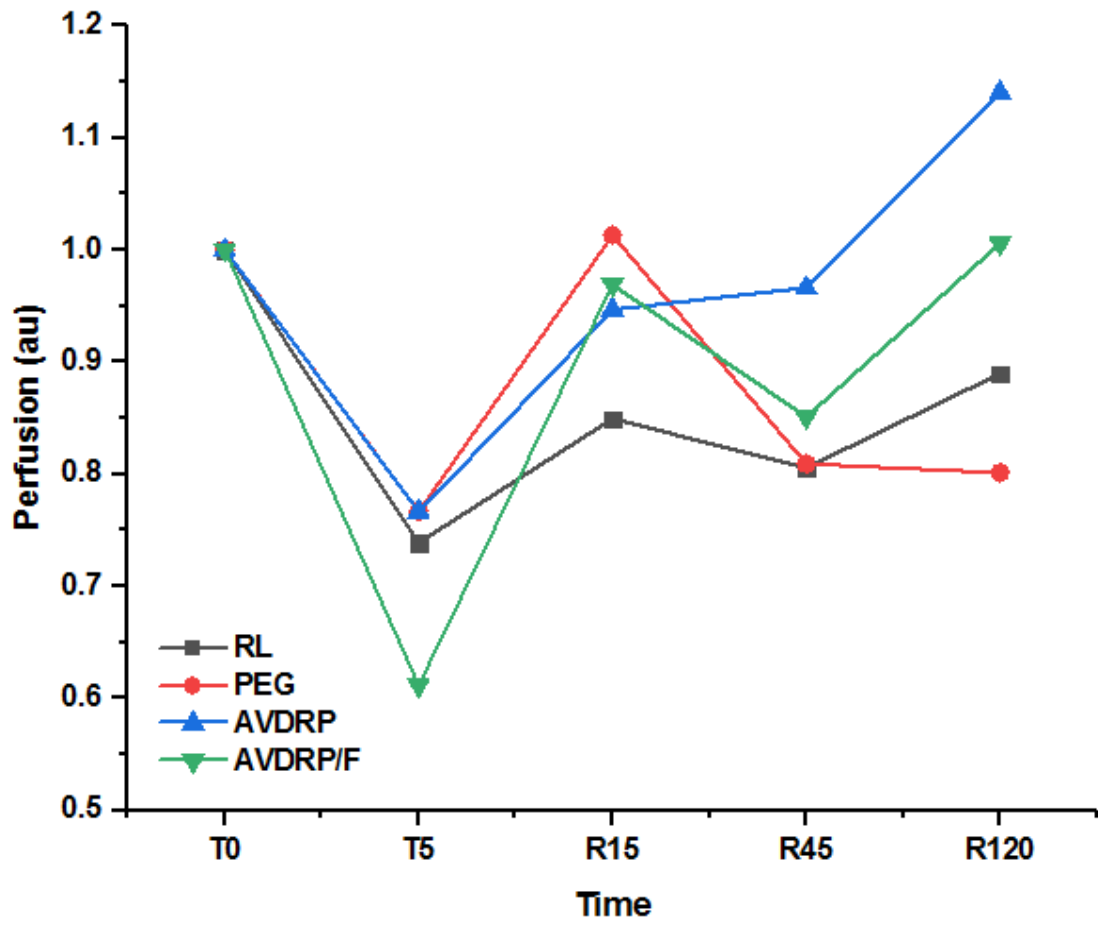
Figure 3.7.2: Laser Speckle Imaging data indicates tissue perfusion among RL, PEG, AVDRP, and AVDRP/F groups (n=8). (Data were normalized to T_0)

Chapter 4

Conclusion

Blood-soluble AVDRP and modified AVDRP/F were effectively investigated and characterized for potential clinical use in hemorrhagic shock and; they were further elucidated in terms of effects on blood circulation, tissue perfusion *in-vivo*. We investigated the resuscitation agents that Ringer Lactate which is a resuscitation agent used in the clinic and commercial PEG, AVDRP which is synthesized from aloe-vera and AVDRP/F which is modified with perfluorocarbon to contribute to tissue oxygenation in terms of drag-reducing potential and tissue perfusion. We demonstrated that DRPs has ppm level concentration were significantly successful in restoring MAP in rabbits subjected to fixed-pressure hemorrhagic shock. Furthermore, we have shown that these DRPs significantly increase blood flow intensity and tissue perfusion with the images and records obtained by laser speckle imaging.

Future work will be aimed at the potential of DRP to be an alternative resuscitation agent will be investigated in a larger animal model.

Bibliography

[1]   G. Gutierrez, H. D. Reines, and M. E. Wulf-Gutierrez, "Clinical review: Hemorrhagic shock," *Crit. Care*, vol. 8, no. 5, pp. 373–381, 2004.

[2]   D. Cherkas, "Traumatic hemorrhagic shock: advances in fluid management.," *Emerg. Med. Pract.*, vol. 13, no. 11, pp. 1–19; quiz 19–20, 2011.

[3]   M. V Kameneva *et al.*, "Blood soluble drag-reducing polymers prevent lethality from hemorrhagic shock in acute animal experiments.," *Biorheology*, vol. 41, no. 1, pp. 53–64, 2004.

[4]   G. S. Martin and P. Bassett, "Crystalloids vs. colloids for fluid resuscitation in the Intensive Care Unit: A systematic review and meta-analysis," *J. Crit. Care*, vol. 50, pp. 144–154, 2019.

[5]   R. I. Perel P, "Colloids versus crystalloids for fluid resuscitation in critically ill patients," no. 3, pp. 1–71, 2011.

[6]   C. Messmer, O. Yalcin, A. F. Palmer, and P. Cabrales, "Small-volume resuscitation from hemorrhagic shock with polymerized human serum albumin," *Am. J. Emerg. Med.*, vol. 30, no. 8, pp. 1336–1346, 2012.

[7]   A. Cotoia, M. V. Kameneva, P. J. Marascalco, M. P. Fink, and R. L. Delude, "Drag-reducing hyaluronic acid increases survival in profoundly hemorrhaged rats," *Shock*, vol. 31, no. 3, pp. 258–261, 2009.

[8]   P. S. Virk, E. W. Merrill, H. S. Mickley, K. A. Smith, and E. L. Mollo-Christensen, "The Toms phenomenon: Turbulent pipe flow of dilute polymer solutions," *J. Fluid Mech.*, vol. 30, no. 2, pp. 305–328, 1967.

[9]   C. S. Wells and J. G. Spangler, "Injection of a drag-reducing fluid into turbulent pipe flow of a Newtonian fluid," *Phys. Fluids*, vol. 10, no. 9, pp. 1890–1894, 1967.

[10]   W.-M. Kulicke, M. Kötter, and H. Gräger, "Drag reduction phenomenon with special emphasis on homogeneous polymer solutions," *Polym. Charact. Solut.*, pp. 1–68, 2005.

[11]   R. Society, "Flow Induced Polymer Chain Extension and Its Relation to Fibrous Crystallization Author (s): M . R . Mackley and A . Keller Source : Philosophical Transactions of the Royal Society of London . Series A ,

Mathematical Published by : Royal Society Stable ," vol. 278, no. 1276, pp. 29–66, 2016.

[12] J. W. Hoyt, "853 8 8," pp. 1–3, 1971.

[13] A. V. Shenoy, "A review on drag reduction with special reference to micellar systems," *Colloid Polym. Sci.*, vol. 262, no. 4, pp. 319–337, 1984.

[14] P. S. Virk, "Drag reduction fundamentals," *AIChE J.*, vol. 21, no. 4, pp. 625–656, 1975.

[15] J. N. Marhefka *et al.*, "Blood soluble polymers for enhancing near-vessel-wall RBC traffic in presence of hemoglobin based oxygen carrier," *Int. J. Eng. Sci.*, vol. 83, pp. 138–145, 2014.

[16] M. V. Kameneva, "Microrheological effects of drag-reducing polymers in vitro and in vivo," *Int. J. Eng. Sci.*, vol. 59, pp. 168–183, 2012.

[17] J. N. Marhefka, P. J. Marascalco, T. M. Chapman, A. J. Russell, and M. V. Kameneva, "Poly(N-vinylformamide) - A drag-reducing polymer for biomedical applications," *Biomacromolecules*, vol. 7, no. 5, pp. 1597–1603, 2006.

[18] C. A. Macias, M. V. Kameneva, J. J. Tenhunen, J. C. Puyana, and M. P. Fink, "Survival in a rat model of lethal hemorrhagic shock is prolonged following resuscitation with a small volume of a solution containing a drag-reducing polymer derived from aloe vera," *Shock*, vol. 22, no. 2, pp. 151–156, 2004.

[19] M. V. Kameneva, M. P. Fink, G. Gutierrez, and S. Fuller, "Hemorrhagic shock, drag-reducing polymers and 'spherical cows' (multiple letters) [2]," *Crit. Care*, vol. 9, no. 3, pp. 304–305, 2005.

[20] C. A. McCloskey, M. V. Kameneva, A. Uryash, D. J. Gallo, and T. R. Billiar, "Tissue hypoxia activates JNK in the liver during hemorrhagic shock," *Shock*, vol. 22, no. 4, pp. 380–386, 2004.

[21] R. L. Smith, E. F. Blick, J. Coalson, and P. D. Stein, "Thrombus production by turbulence," *J. Appl. Physiol.*, vol. 32, no. 2, pp. 261–264, 2017.

[22] P. B. Coleman, B. T. Ottenbreit, and P. I. Polimeni, "Effects of a drag-reducing polyelectrolyte of microscopic linear dimension (Separan AP-273) on rat hemodynamics," *Circ. Res.*, vol. 61, no. 6, pp. 787–796, 1987.

[23] J. J. Pacella *et al.*, "Modulation of Pre-Capillary Arteriolar Pressure with Drag-Reducing Polymers: A Novel Method for Enhancing Microvascular Perfusion," *Microcirculation*, vol. 19, no. 7, pp. 580–585, 2012.

[24] H. L. Greene, R. F. Mostardi, and R. F. Nokes, "Effects of drag reducing polymers on initiation of atherosclerosis," *Polym. Eng. Sci.*, vol. 20, no. 7, pp. 499–504, 1980.

[25] I. A. Sokolova, A. A. Shakhnazarov, S. N. Sergeev, D. V. Davydov, and V. S. Baranov, "Prophylactic and corrective action of the polyethylene oxide polyox WSR-301 in rats with experimental lipoidosis," *Bull. Exp. Biol. Med.*, vol. 119, no. 6, pp. 564–567, 1995.

[26] J. N. Marhefka, R. Zhao, Z. J. Wu, S. S. Velankar, J. F. Antaki, and M. V. Kameneva, "Drag reducing polymers improve tissue perfusion via modification of the RBC traffic in microvessels," *Biorheology*, vol. 46, no. 4, pp. 281–292, 2009.

[27] O. F. The, "hundred years have passed since the French physician Poiseuille (1) took up for consideration the important problem of the resistance," no. 8, pp. 562–568, 1930.

[28] H. L. Goldsmith and S. Spain, "Margination of leukocytes in blood flow through small tubes," *Microvasc. Res.*, vol. 27, no. 2, pp. 204–222, 1984.

[29] P. J. Marascalco, H. C. Blair, A. Nieponice, L. J. Robinson, and M. V. Kameneva, "Intravenous injections of soluble drag-reducing polymers reduce foreign body reaction to implants," *ASAIO J.*, vol. 55, no. 5, pp. 503–508, 2009.

[30] A. Fülöp, Z. Turóczi, D. Garbaisz, L. Harsányi, and A. Szijártó, "Experimental models of hemorrhagic shock: A review," *Eur. Surg. Res.*, vol. 50, no. 2, pp. 57–70, 2013.

[31] "Artificial oxygen carriers," *Eur. J. Anaesthesiol.*, vol. 15, no. 5, pp. 571–584, 1998.

[32] D. R. Spahn, "Blood substitutes: Artificial oxygen carriers: Perfluorocarbon emulsions," *Crit. Care*, vol. 3, no. 5, pp. 93–97, 1999.

[33] P. CABRALES, B. Y. S. VÁZQUEZ, A. C. NEGRETE, and M. INTAGLIETTA, " Perfluorocarbons as gas transporters for O 2 , NO, CO and volatile anesthetics ," *Transfus. Altern. Transfus. Med.*, vol. 9, no. 4, pp. 294–303, 2008.

[34] J. L. Lomas-Niera, M. Perl, C. S. Chung, and A. Ayala, "Shock and hemorrhage: An overview of animal models," *Shock*, vol. 24, no. SUPPL. 1, pp. 33–39, 2005.

[35] K. Eshun and Q. He, "Aloe Vera: A Valuable Ingredient for the Food, Pharmaceutical and Cosmetic Industries - A Review," *Crit. Rev. Food Sci. Nutr.*, vol. 44, no. 2, pp. 91–96, 2004.

[36] J. Tai-Nin Chow, D. A. Williamson, K. M. Yates, and W. J. Goux, "Chemical characterization of the immunomodulating polysaccharide of Aloe vera L.," *Carbohydr. Res.*, vol. 340, no. 6, pp. 1131–1142, 2005.

[37] B. Y. J. Armin, R. T. Grant, H. Pels, and E. B. Reeve, "ALBINO RABBITS AS ESTIMATED BY THE DYE (T 1824) AND UP MARKED CELL METHODS From The Clinical Research Unit , Guy ' s Hospital , London At present the most satisfactory estimates of blood volume are obtained from summing simultaneous

measurements ofplasm," no. T 1824, pp. 59–73, 1951.

[38] A. Surjushe, R. Vasani, and D. Saple, "Aloe vera: A short review," *Indian J. Dermatol.*, vol. 53, no. 4, pp. 163–166, 2008.

[39] J. Marhefka and M. Kameneva, "Natural Drag-Reducing Polymers: Discovery, Characterization and Potential Clinical Applications," *Fluids*, vol. 1, no. 2, p. 6, 2016.

[40] Amanda R. Daly, Hideo Sobajima, Salim E. Olia, Setsuo Takatani and M. V. Kameneva, "Application of Drag-Reducing Polymer Solutions as Test Fluids for In Vitro Evaluation of Potential Blood Damage in Blood Pumps," *NIH Public Access*, vol. 56, no. 1, pp. 6–11, 2010.

[41] Y. I. Cho and J. P. Harnett, "Non-Newtonian Fluids in Circular Pipe Flow," *Adv. Heat Transf.*, vol. 15, no. C, pp. 59–141, 1982.

[42] Joie Nicole Marhefka, "STUDY OF DRAG REDUCING POLYMERS AND MECHANISMS OF THEIR INTRAVASCULAR EFFECT," *PHD Thesis*, vol. 7, no. 3, pp. 213–221, 2007.

[43] L. Benato, M. Chesnel, K. Eatwell, and A. Meredith, "Arterial blood gas parameters in pet rabbits anaesthetized using a combination of fentanyl-fluanisone-midazolam-isoflurane," *J. Small Anim. Pract.*, vol. 54, no. 7, pp. 343–346, 2013.

[44] M. Ardiaca, C. Bonvehí, and A. Montesinos, "Point-of-Care Blood Gas and Electrolyte Analysis in Rabbits," *Vet. Clin. North Am. - Exot. Anim. Pract.*, vol. 16, no. 1, pp. 175–195, 2013.

[45] G. Chen, L. Zhao, Y. W. Liu, F. L. Liao, D. Han, and H. Zhou, "Regulation of blood viscosity in disease prevention and treatment," *Chinese Sci. Bull.*, vol. 57, no. 16, pp. 1946–1952, 2012.

[46] C. Y. Wu, Y. C. Yeh, C. T. Chien, A. Chao, W. Z. Sun, and Y. J. Cheng, "Laser speckle contrast imaging for assessing microcirculatory changes in multiple splanchnic organs and the gracilis muscle during hemorrhagic shock and fluid resuscitation," *Microvasc. Res.*, vol. 101, pp. 55–61, 2015.

ALOE VERA EXTRACT AS DRAG REDUCING POLYMER TO REGULATE BLOOD PRESSURE AND TISSUE OXYGENATION DURING HEMORRHAGIC SHOCK